SSC San Diego Biennial Review 2003

2

# Communication and Information Systems

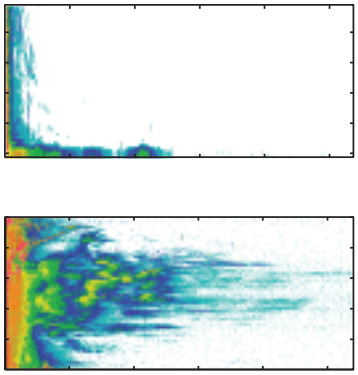

# Report Documentation Page

*Form Approved*
*OMB No. 0704-0188*



| 1. REPORT DATE | 2. REPORT TYPE | 3. DATES COVERED |
|---|---|---|
| **2003** | | **-** |

| 4. TITLE AND SUBTITLE | 5a. CONTRACT NUMBER |
|---|---|
| **SSC San Diego Biennial Review 2003. Communication and Information Systems** | 5b. GRANT NUMBER |
| | 5c. PROGRAM ELEMENT NUMBER |
| 6. AUTHOR(S) | 5d. PROJECT NUMBER |
| | 5e. TASK NUMBER |
| | 5f. WORK UNIT NUMBER |
| 7. PERFORMING ORGANIZATION NAME(S) AND ADDRESS(ES) **Space & Naval Warfare Systems Center,53560 Hull St,San Diego,CA,92152-5001** | 8. PERFORMING ORGANIZATION REPORT NUMBER |
| 9. SPONSORING/MONITORING AGENCY NAME(S) AND ADDRESS(ES) | 10. SPONSOR/MONITOR'S ACRONYM(S) |
| | 11. SPONSOR/MONITOR'S REPORT NUMBER(S) |

12. DISTRIBUTION/AVAILABILITY STATEMENT
**Approved for public release; distribution unlimited**

13. SUPPLEMENTARY NOTES
**The original document contains color images.**

14. ABSTRACT
**see report**

15. SUBJECT TERMS

| 16. SECURITY CLASSIFICATION OF: | | | 17. LIMITATION OF ABSTRACT | 18. NUMBER OF PAGES | 19a. NAME OF RESPONSIBLE PERSON |
|---|---|---|---|---|---|
| a. REPORT | b. ABSTRACT | c. THIS PAGE | | | |
| **unclassified** | **unclassified** | **unclassified** | | **49** | |

# Lessons (Innovations) in Technology Transfer

**Stephen E. Stewart, Stephen Lieberman, Stephen D. Russell, and Matt McLandrich**
SSC San Diego

ABSTRACT

***This paper describes different approaches to the technology transfer of SSC San Diego-developed technologies to commercial and government markets. Several case studies are presented in which various technology-transfer tools including Cooperative Research and Development Agreements (CRADAs), exclusive and non-exclusive licensing agreements, were used to spin out government-developed technology to the commercial market. Case studies include (1) an improved micro-display technology using an ultra-thin crystalline layer of silicon (less than 200 atoms thick) on a transparent sapphire substrate that offers improved imaging and video in virtual-reality displays and in advanced hand-held information technology devices, (2) fused fiber-optic wavelength division multiplexers (WDMs) capable of combining light in two wavelength bands onto a single fiber and later separating light in these wavelength bands for detection, and (3) an automated oil-spill detection system designed to provide early detection and notification of a petroleum spill on water. For each technology, details of the technology-transfer process are presented and benefits to the Department of Defense and dual-use commercial markets are documented.***

## INTRODUCTION

The greatness of the United States is built, in part, on its technology base and innovative technology development. Over the past several decades, the government has worked to promote technology development throughout our society. One such avenue is the transfer to the private sector and commercialization of government-developed technology. In 1980, legislation required each federal laboratory to establish an Office of Research and Technology Applications (ORTA) to coordinate and promote technology transfer. Congress officially chartered the Federal Laboratory Consortium (FLC) for Technology Transfer in 1986 and enabled government laboratories to enter into Cooperative Research and Development Agreements (CRADAs) and to negotiate licensing arrangements with industry for laboratory patents. Subsequent laws have expanded the scope of this basic technology-transfer structure, eased restrictions on its application, and made participation more attractive to both government and industry.

In 2001, Congress provided funding to establish the Center for Commercialization of Advanced Technology (CCAT) in San Diego. The CCAT is a partnership between SSC San Diego, San Diego State University Foundation and Entrepreneurial Management Center, the University of California, San Diego (UCSD) CONNECT and UCSD Jacobs School of Engineering, and Orincon Technologies International to fast-track Department of Defense (DoD), industry, and academic technologies into dual-use commercial and defense start-up ventures and to promote technology insertion into existing companies. Whereas FLC programs and CRADAs provide no government funding for transfer efforts—any flow of funds being only from industry to government laboratories—CCAT provides funds to government laboratories, industry, and academia to facilitate the transfer and commercialization of technology.

The benefits of technology transfer and commercialization to all parties are substantial. Industry gains another source of new technology and product ideas and can realize considerable savings for research and development that have already been accomplished at government laboratories and academic institutions. The DoD is offered the potential of obtaining the economies of scale of the commercial market along with the additional funding of commercial investors. Academia enters into closer

partnerships with government and industry and gains increased potential to receive additional funding for basic research.

## CASE STUDIES

We present three case studies from technologies developed at SSC San Diego that were spun out to the commercial market, illustrating the mechanisms and benefits of technology transfer and commercialization.

### Micro-Display

Our first case study deals with the transfer of manufacturing-process technology for a novel, high-performance, active-matrix, liquid-crystal micro-display formed on an ultra-thin layer of silicon-on-sapphire (SOS). SSC San Diego scientists and engineers invented and demonstrated a display manufacturing technique by using an ultra-thin layer (less than 200 atoms thick) of crystalline silicon on a transparent sapphire substrate [1]. This technique allowed the fabrication of high-performance microelectronic circuitry within and adjacent to a liquid crystal display. This method produces a high-resolution and high-brightness display and eliminates the need for millions of wire interconnections, thereby improving performance, manufacturability, and reliability. Specific features of the technology include low-power operation and very high speed due to reduced parasitic capacitance of the SOS microcircuits, monolithic integration of control circuitry that avoids interconnect problems, high brightness by reducing the size of the pixel transistors, and high resolution by using rapidly switched field sequential color schemes that eliminate the need for red-green-blue subpixels. The micro-display technology offers improved imaging and video in virtual-presence applications for the warfighter and emergency service personnel (police, firefighters, paramedics, etc.) and in small advanced information-technology devices such as hand-held or wearable computers and cellular phones.

The technology-transfer process involved a coalition of government and industrial partners, each providing important contributions. The inventors initiated the technology-transfer effort and collaborated on technical development; the SSC San Diego ORTA coordinated multiple CRADAs; the SSC San Diego Patent Counsel supported the protection of intellectual property, filed and prosecuted patent applications, and negotiated the Navy license; Proxima Corporation supported development of a technology roadmap and identified product opportunities; and Optron Systems, Inc., and Radiant Images, Inc., were the recipients of the technology.

The technology-transfer process began by modeling the expected performance and advantages of the invention, which enabled credible marketing to potential industry partners. This step was followed by an initial CRADA with Proxima Corporation. The goal of the Proxima CRADA was to identify insertion opportunities for the emerging technology and assist in marketing to U.S. display-component manufacturers. Through the Proxima CRADA, predictions of market size and technology viability then enabled collaborative marketing to the display-component manufacturer, Optron Systems, Inc. A subsequent CRADA with Optron Systems provided the mechanism to jointly fabricate a "proof-of-concept" micro-display. A 1/4-sized video graphics array (VGA) display (Figure 1) provided the mechanism to effectively market the invention to venture capitalists to facilitate commercialization of the technology.

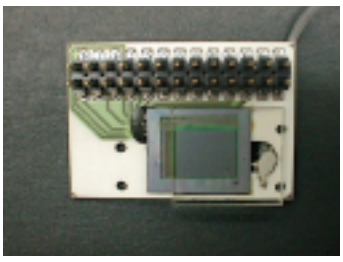

FIGURE 1. First-generation monochrome 1/4-VGA micro-display.

A license agreement was completed between the U.S. Navy, represented by SSC San Diego, and Optron Systems for the exclusive rights to U.S. patents. The government has now successfully transitioned the technology, and Optron Systems has spun-off a new company (Radiant Images, Inc.) to produce the micro-displays as a domestic source of micro-displays for original equipment manufacturers. Figure 2 shows the second-generation full-color SVGA micro-display that has pixels with a 12-micrometer pitch (a human hair is approximately 50 micrometers wide), and a display size of approximately 0.5 inch diagonally. Radiant Images produced this display by using the SSC San Diego technology that is now commercially available.


FIGURE 2. Second-generation full-color SVGA micro-display.

## Fused Fiber-Optic Coupler

An important function in fiber-optic communications networks is wavelength division multiplexing (WDM). WDM allows multiple optical signals at different wavelengths to be combined onto a single fiber for simultaneous transmission and then to be separated for detection at the receiver. WDM devices can also drop or add one or more wavelength channels on a multiplexed link and perform wavelength routing, whereby certain channels are directed along selected optical paths in the link. Thus, WDM enables enhanced fiber-optic communications systems by increasing information capacity (bandwidth) and architectural flexibility.

SSC San Diego has concentrated its WDM research and development (R&D) efforts on a specific type of device: the fused fiber-optic coupler [2]. The fiber coupler consists of two single-mode fibers that have been fused together, tapered, and elongated along a common length, typically on the order of 1 to 2 centimeters. Figure 3 shows sections of a fused fiber coupler schematically and in photomicrographs. Original input fibers with diameters of 125 microns are reduced to a fused section with cross-sectional size on the order of a few tens of microns. Fused fiber pairs act as a coupler because part or all of the power in an optical signal launched into one of the fibers will transfer into the second fiber, depending on such things as the cross-sectional dimensions and shape of the fused fibers and the length of the fused region. With the right dimensions, light of one wavelength will completely couple from the original input fiber to the second fiber, while light of a second wavelength will completely couple from the original fiber to the second fiber and then back to the original fiber. Thus, two signals on one fiber entering the fused region are demultiplexed onto different output fibers. Also, because the coupling process is reciprocal, the same coupler acts as a multiplexer. Combining couplers with the appropriate wavelength-transfer functions into a tree structure enables multiplexing and demultiplexing of any number of channels. The wavelength channel spacing can be as small as a few nanometers up to hundreds of nanometers. The same types of couplers can also be configured to implement wavelength add-and-drop and selective routing functions.

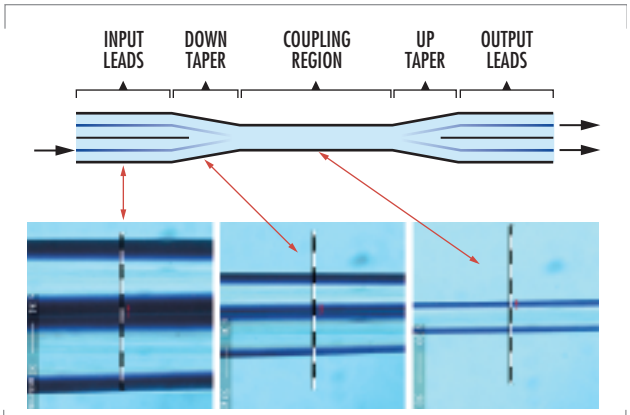


FIGURE 3. Schematic of fused fiber coupler and typical photomicrographs at input leads, down taper, and coupling region.

While simple in concept, the fused fiber WDM coupler is difficult to fabricate with high yield. Coupler dimensions must be controlled to within a

few microns, and optical loss in the device must be held to the order of a few tenths of a decibel or less. Other effects, such as the sensitivity to varying states of polarization of the input signal also must be considered in the design and fabrication of the coupler. SSC San Diego developed a computer-controlled fused fiber fabrication station to achieve the required precision in coupler fabrication and a resulting high production yield. In combination with precision motorized translation stages, the computer controls the positioning of the fibers and a micro-torch for fusing, and the elongation of the fibers during fusing. Also, by launching an optical signal into one of the fibers and monitoring the outputs that are fed to the computer, the fusion process can be controlled, adjusted, and stopped at precisely the exact point to obtain the specified coupling conditions.

SSC San Diego has several patents covering the design and fabrication of fused fiber couplers that use automated computer-controlled fabrication techniques. Various companies, realizing the potential benefit of this technology, expressed interest in acquiring patent licenses. SSC San Diego researchers, working with the Center's Patent Office, negotiated and drafted reasonable and fair non-exclusive patent licenses and concurrent CRADAs with six companies, ranging from small start-ups to large internationals. The CRADAs are the primary vehicles by which all of the coupler-fabrication technology developed at SSC San Diego is transferred to the companies. The material includes equipment specifications, engineering drawings, computer software, process procedure instructions, hands-on training, and continuing consultation. Several companies have developed prototype devices, and some are using the fused coupler technology to support in-house R&D programs. Finally, because the patent licenses are non-exclusive, the opportunity exists for other companies to acquire the SSC San Diego fused fiber WDM coupler technology on the same licensing terms and to receive the technology transfer through CRADAs.

### Oil-Spill Detection

Rapid, reliable spill detection is an essential yet often overlooked part of oil-spill prevention and response strategies. Early detection of a petroleum leak or spill enables responders to take immediate actions to stop and contain the released material. By enhancing the ability to exercise timely countermeasures, early detection offers an effective means of minimizing the environmental and financial impact of a spill. On the other hand, a failure or delay in recognizing the existence of a spill leads to a delayed response, which may result in a larger spill volume and costlier cleanup effort. Current oil-spill detection methods rely solely on human observation to identify the presence of a spill—a very unreliable practice. To address this issue, the SSC San Diego team developed an automated spill-sensing technology.

The automated technology provides early notification of a petroleum spill on water. The fluorescence-based sensor operates just below the water surface and continuously tests for an increased hydrocarbon concentration, which is indicative of a spill. When a spill is detected, a radio signal is immediately transmitted to a base-station computer for analysis, display, and electronic alarming. Once a spill has been detected, responders immediately receive an automated phone call that alerts them.

To transfer the technology, an SSC team led by John Andres entered into an exclusive licensing agreement with Applied Microsystems Ltd. (AML), a Canadian company that designs and manufactures water-quality monitoring instrumentation. Currently, AML is globally marketing the detection system under the name "Spill Sentry" (buoy shown in Figure 4). Since the technology was licensed to a Canadian company, special provisions were negotiated in the licensing agreement to ensure benefit to the U.S. economy. The commercial product has recently undergone a spin into the DoD with several units installed at DoD facilities in Puget Sound Naval Shipyard, Langley Air Force Base, Naval Station Norfolk, Naval Station Pearl Harbor, and Naval Station San Diego. In addition, the commercial unit was recently modified to include bioluminescence sensors for real-time continuous measurement of stimulated bioluminescence in coastal environments.

FIGURE 4. Photograph of buoy-mounted oil-spill detection system.

REFERENCES

1. Shimabukuro, R. L., S. D. Russell, and B. W. Offord. 1994. "Ultra-Thin Silicon-on-Sapphire for High-Density AMLCD Drivers," *SPIE Proceedings*, vol. 2174, February, pp. 82–90.
2. McLandrich, M. N., R. J. Orazi, and H. R. Marlin. 1991. "Polarization Independent Narrow Channel Wavelength Division Multiplexing Fiber Couplers for 1.55 Microns," *Journal of Lightwave Technology*, vol. 9, no. 4, pp. 442–447.

**Stephen E. Stewart**
Ph.D., Physics, Brigham Young University, 1979
Current Research: Technology development planning for SSC San Diego.

**Stephen Lieberman**
Ph.D., Chemical Oceanography, University of Washington, 1979
Current Research: Optical-based chemical sensors and sensor systems; bacteriophage-based recognition systems for biological agents.

**Stephen D. Russell**
Ph.D., Physics, University of Michigan, 1986
Current Research: Microsensors; photonic devices; opto-electronics; micro-electronics; micro-electro-mechanical systems (MEMS); laser applications.

**Matt McLandrich**
MS, Physics, San Diego State University, 1974
Current Research: Fused fiber couplers; wavelength division multiplexing; fiber Bragg grating fabrication.

# Combined Operations Wide Area Network (COWAN)/Combined Enterprise Regional Information Exchange System (CENTRIXS)

**Brad Carter and Deb Harlor**
SSC San Diego

ABSTRACT

*This paper discusses the continued development and operation of the Combined Operations Wide Area Network (COWAN) in support of U.S. Pacific Command's initiative to provide classified, permanent network service for bilateral and multilateral communities of interest for combined and coalition operations. The COWAN project, headed by SSC San Diego personnel, continues to grow and has recently been consolidated with the Combined Enterprise Regional Information Exchange System (CENTRIXS) program, originally designed to support U.S. Central Command requirements. The consolidation of these efforts has created a dynamic team of personnel working to meet the increasing need for secure global connectivity. Challenges continue to confront the team, primarily in getting approved and accredited technical solutions for connecting multiple classified domains to facilitate the War on Terrorism.*

## BACKGROUND

Numerous coalition wide area networks (CWANs) have been built by operational commanders to support coalition operations and exercises, only to be dismantled at the completion of the objectives. This process is inefficient, requiring a long lead-time for planning and implementation. This paradigm limits the commander's ability to streamline tactics, techniques, and procedures for coalition information exchange.

SSC San Diego's role has been threefold. First, SSC San Diego developed the Combined Operations Wide Area Network (COWAN) for Commander, Pacific Fleet (COMPACFLT) and subsequently became the Navy's representative to coalition networking under the Combined Enterprise Regional Information Exchange System (CENTRIXS) program. Second, SSC San Diego has been the technical advisor to COMPACFLT in its role as Executive Agent for coalition networking under Commander, Pacific Command (CDR USPACOM). This effort includes establishing a joint global coalition network architecture as part of the Global Information Grid in coordination with the Office of the Assistant Secretary of Defense/Command, Control, Computers, and Intelligence (ASD C3I) CENTRIXS Program Office, as well as representatives from U.S. Central Command (CENTCOM), U.S. European Command (EUCOM), and U.S. Southern Command (SOUTHCOM). Third, SSC San Diego's Network Centric Computing program has joined both COMPACFLT and PACOM in technology insertion efforts to demonstrate thin client technology with high-assurance network access and data separation to provide a single workstation access to multiple communities of interest (COIs).

## HISTORY

In the PACOM area of responsibility, COMPACFLT, with SSC San Diego technical support, developed the first maritime CWAN in support of the Rim of the Pacific Exercise 1998 (RIMPAC 1998). This initial effort consisted of secure email using Secure Telephone Units-Third Generation (STU-IIIs) over a 2.4K International Maritime Satellite (Inmarsat) channel. Follow-on efforts expanded the functionality to allow passing of email between the Secret Internet Protocol Router Network (SIPRNET) and the CWAN through a secure mail guard, and also allowed for the sharing of data through Web browsing. This expanded capability was demonstrated during RIMPAC 2000 and Exercise Tandem

Thrust 2001, using super high-frequency and Inmarsat B connections. The CWAN architecture during Tandem Thrust 2001 allowed U.S. and Australian headquarters to communicate on a variety of levels with maritime, ground, and air component commanders. To maintain this connectivity after the exercise, COMPACFLT achieved a 3-year Department of Defense Security and Accreditation Working Group approval for the mail guard between SIPRNET and the coalition network, renamed COWAN-A. The COWAN-A network supported Australia, Canada, the United Kingdom, and the United States.

USPACOM determined in 2001 that there was a need to consolidate coalition network development and provide a way ahead within the theater. Making use of COMPACFLT's expertise in coalition networks, PACOM selected PACFLT as the Executive Agent for this task. In April 2001, PACFLT N6, supported by SSC San Diego, began working as PACOM's Executive Agent for coalition networking. The original goal was to demonstrate the utility of establishing permanent, classified network service with Pacific Rim partner nations to more quickly establish a Joint Task Force Commander's command and control when required. In this manner, COWAN-T was stood up and used by the III Marine Expeditionary Force to revolutionize coalition warfighting during Exercise Cobra Gold 2002, by fighting principally on the COWAN vice SIPRNET/Non-Secure Internet Protocol Router Network (NIPRNET). In addition to Cobra Gold, much of the COWAN effort by SSC San Diego included expanding COWAN-A, as it soon became the primary coalition network supporting Operation Enduring Freedom.

In 2001, the office of ASD C3I and CENTCOM fielded a global multinational information-sharing network called CENTRIXS. This was followed in January 2002 by ASD C3I's establishment of the CENTRIXS program management office to expand coalition networks in support of Operation Enduring Freedom.

In October 2002, SSC San Diego implemented PACOM theater remote access to CENTCOM's CENTRIXS-Global Counter Terrorism Force (GCTF) community of interest (50+ nations) to support liaison officers, staff, and deployed or mobile units in support of Operation Enduring Freedom.

In February 2003, COWAN and a PACOM intelligence-sharing program known as Pacific Bilateral Intelligence Information Exchange System changed names to CENTRIXS to begin efforts to standardize regional networks, leverage functionality, and provide standard software configurations, information assurance, and concept of operations.

Figure 1 shows the COWAN overview.

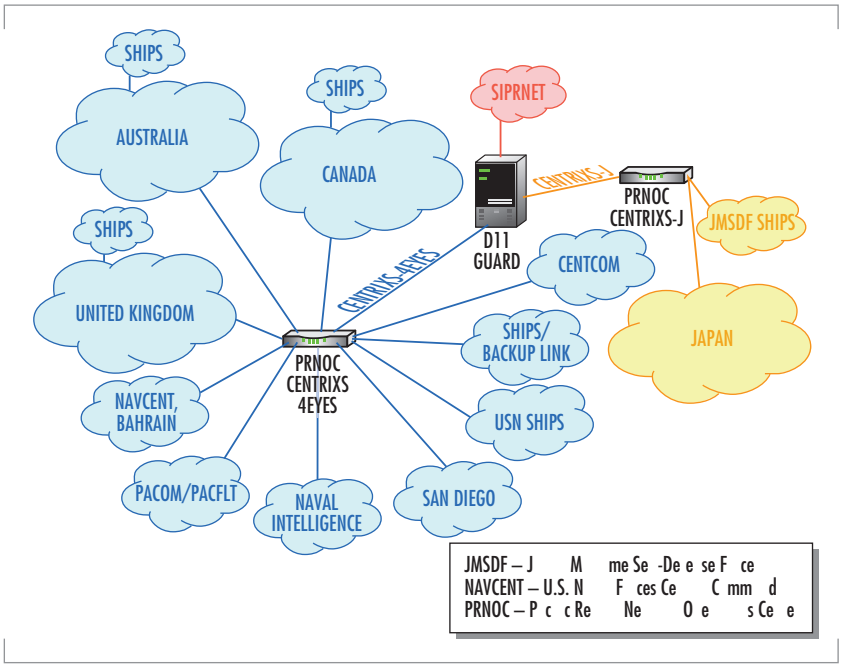


FIGURE 1. COWAN overview.

## CURRENT NETWORKING APPROACH (TECHNICAL REQUIREMENTS)

Coalition operations demand responsive information exchange across combined forces and unified commands for planning, unity of effort, decision superiority, and decisive global operations. The CENTRIXS and COWAN networks now support this operational requirement.

The primary CENTRIXS networks include CENTRIXS-4EYES (previously COWAN-A) and CENTRIXS-J (U.S./Japan). These networks initially provided connectivity with coalition maritime forces and with each country's maritime headquarters. CENTRIXS-4EYES, however, has been expanding into the joint arena in the U.S. and the other participating nations. For the maritime platforms, connectivity is made over Inmarsat dial-up, while the major allied shore commands have dedicated circuits. The U.S. users, including afloat units, use TACLANE tunneling over SIPRNET. CENTRIXS-4EYES and CENTRIXS-J use a secure mail guard and provide web data via Lotus Domino™ using an air-gap routine for two-way data exchange between the COWAN enclaves and SIPRNET. CENTRIXS-4EYES has CHAT (conversational hypertext access technology) and a common operational picture, which is not currently available on CENTRIXS-J. CHAT capability is the most operationally significant function on CENTRIXS-4EYES and is extensively used for operational coordination.

CENTRIXS is web-centric and commercial off-the-shelf oriented. Core information services include email with attachments, Web browser data access, and file sharing. Information transfer employs information technology to support responsive movement of approved data from U.S. sources. This includes email guards for email, specialty guards for formatted message text data, and one-way feed for file and database transfers.

Figure 2 shows the CENTRIXS architecture.

The system is intended to support multilateral information sharing as well as specific COIs. The CENTRIXS-GCTF network at CENTCOM supports more than 50 nations. Other CENTRIXS networks have been installed to support bilateral agreements for specific COIs.

The ASD C3I CENTRIXS program office is currently merging the COWAN networks with CENTRIXS. Both networks provide the same basic functionality. The primary difference between the two networks is the use of CHAT and Domino replication on COWAN. CHAT is used to support the rapid dissemination

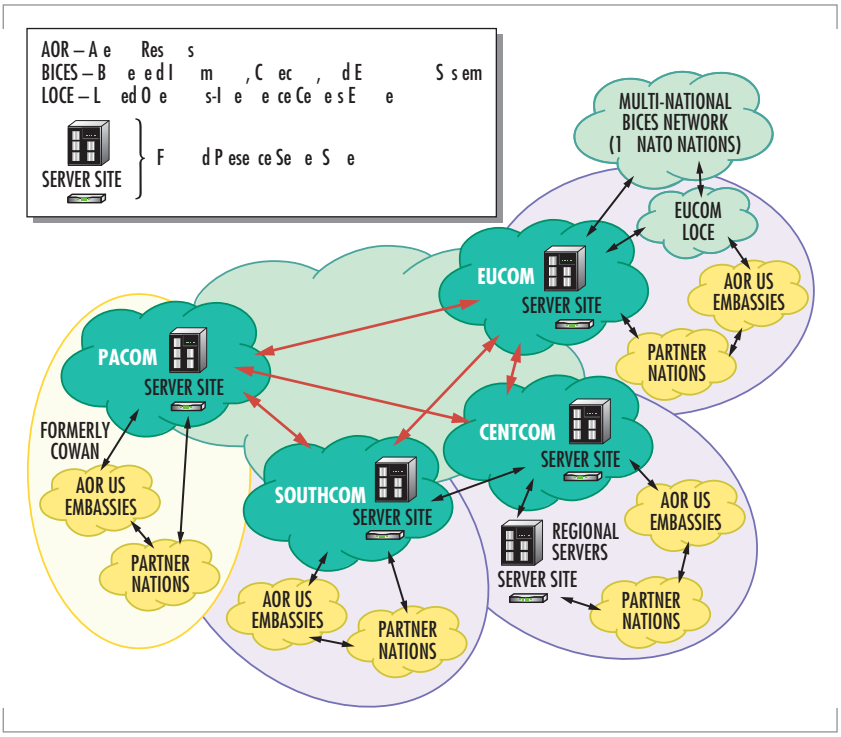


FIGURE 2. CENTRIXS architecture.

of time-critical information. The inability to use CHAT between different classified domains requires U.S. ships to have both SIPRNET and CENTRIXS networks to coordinate with U.S. and coalition forces. Because of limited bandwidth available to ships, Domino replication has been selected as the standard for collaboration at sea.

## CURRENT AND FUTURE EFFORTS

The Coalition Warfare Program (CWP) COWAN/CENTRIXS effort is an Office of the Secretary of Defense/PACOM-sponsored Joint Warfighter Interoperability Demonstration 2003 (JWID 2003) coalition interoperability trial to demonstrate a dynamic coalition network and security solution. Currently being developed by the Space and Naval Warfare Systems Command (SPAWAR) and industry, CWP uses network-centric computing technologies, ultra thin clients, smart cards, and Cryptek™ evaluation assurance level 4 (EAL 4)-certified virtual private network (VPN) devices to create networks that are flexible and secure. The main focus is to provide enhanced capability on a single workstation and ensure that the right information gets to the right person, at the right place, at the right time.

Initial efforts to develop an accredited VPN device were demonstrated in JWID 2002. Using a non-classified local-area network with an ultra thin client architecture, PACOM showcased the ability to simultaneously access separate COIs with privacy. As a follow-on, in JWID 03 PACOM is sponsoring a classified interoperability trial focusing on agile VPN as the key to providing privacy within a coalition. This demonstration will be run on the classified Combined Federated Battle Labs Network (CFBL) located within five countries.

Figure 3 shows the JWID architecture overview.

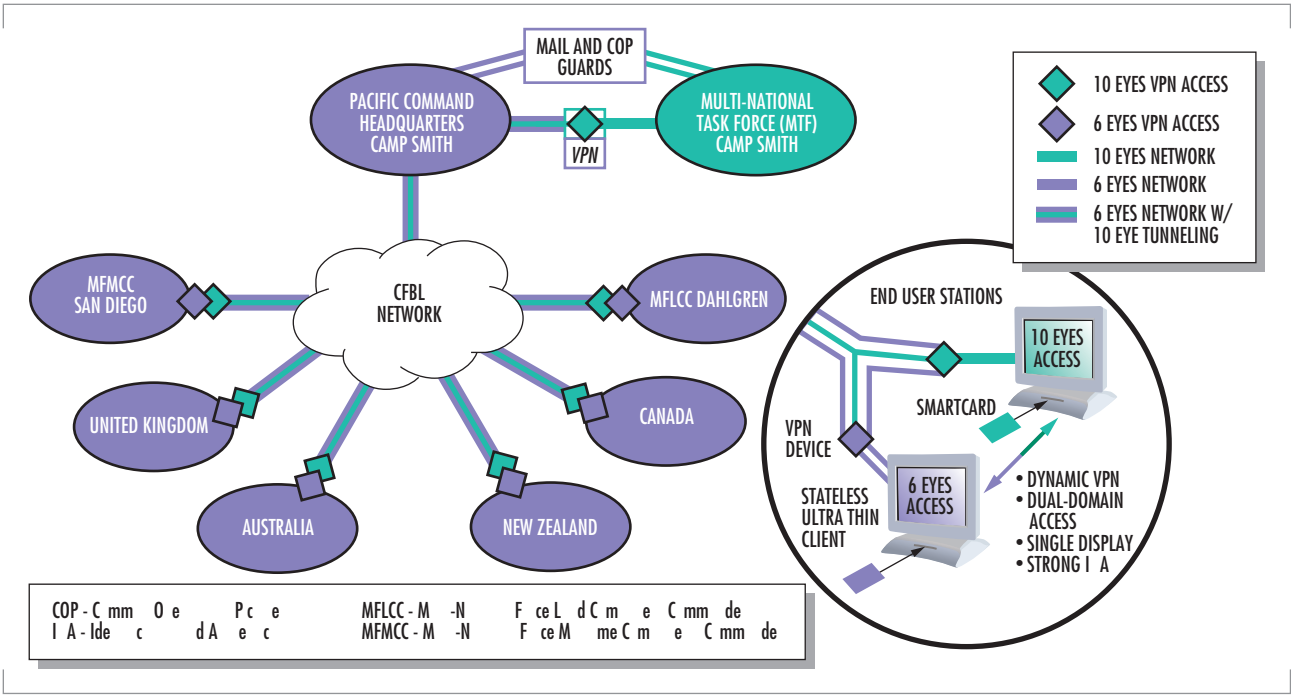


FIGURE 3. JWID architecture overview.

Preliminary analysis indicates that the National Security Agency (NSA) will likely endorse accreditation of PACOM's JWID wide-area network implementation with data separation between communities, provided by a Cryptek VPN device. In terms of functionality, Defense Information Infrastructure (DII) mail guards and Radiant Mercury multilevel security guards will be used to automate and safeguard email and common operational picture services. Collaboration implementation is limited because thin clients lack Internet Protocol (IP) addresses. CHAT and other collaboration tools will be demonstrated by leaving a fat client on the JWID 03 network to act as the host for the collaboration sessions.

Long-term goals are to insert a Type-1 version of the Cryptek VPN device. Cryptek has a memorandum of agreement with the NSA and has produced preliminary design and system requirements specifications documents. This effort's schedule depends on publication of the High Assurance Internet Protocol Encryptor System (HAIPES) II specification by the NSA. Of interest, the HAIPES specification brings definition of over-the-network key (which provides one of the bases for agile algorithm VPN, a Type-1 algorithm for U.S. use, and a Type-1 algorithm AES [Advanced Encryption System] for coalition use). Other future enhancements in the Cryptek product are integrated user identification and authentication (common access card and biometrics) and enhanced system management with centralized policy definition, audit reporting, system updates, and status monitoring.

## AUTHOR INFORMATION

**Brad Carter**

BA, Sociology/Statistics, University of Puget Sound, 1975

Current Work: CENTRIXS (COWAN) Project Manager at PACFLT, N6.

**Deb Harlor**

MS, Information Management, Hamilton University, 2002

Current Work: Integration/ Interoperability Manager, CENTRIXS Lead at USPACOM, J6.

# Joint Distance Support and Response (JDSR): An Approved FY 02–06 Advanced Concept Technology Demonstration (ACTD)

**Ahn Nuzen**
SSC San Diego

**Bill Taw**
Crane Division, Naval Surface Warfare Center

ABSTRACT

***The Joint Distance Support and Response (JDSR) system is an approved FY 02–06 Advanced Concept Technology Demonstration (ACTD). The JDSR system will be developed and tested over the first 3 years with an extended user evaluation in FY 05–06. The implementation of JDSR consists of leveraging and augmenting the technologies and infrastructures of ongoing telemaintenance development programs across the armed services. This will create a common joint operational concept for near-real-time reachback and response from subject matter experts and authoritative data sources. The conceptual approach uses telecommunication and the integration of technologies to focus on the timely employment of information/data to the different service maintainers under various deployed scenarios. JDSR will provide the services with four integrated functions: remote collaboration, information/knowledge sharing, remote platform diagnostics, and distant training/maintenance mentoring.***

## BACKGROUND

The military faces a host of demanding challenges. The environment of fast-paced technology change and rapid modernization, and the support of an ever-increasing number of missions with a declining budget, has forced the military to seek out savings and make infrastructure changes. This has led to reductions in both deployed support forces and organic support structure, forcing the services to do business differently. Maintainers are supporting more complicated and technically sophisticated systems in greater numbers, with fewer personnel and/or limited training.

The services recognize that maintenance and training information must be provided when and where it is needed in the warfare environment and during operations. With timely employment of information, the logistics footprint and the number of maintenance personnel can be reduced while maintaining current or increased levels of required support. Joint Vision 2020 also points to the use of a network-centric environment with a virtual presence for support.

As commercial-off-the-shelf (COTS) technology has matured, extensive work has been done to enable the maintainer to use management information systems, information portals, automatic information technology, wireless technology, communications technology, and electronic tools for global reach to information and subject matter experts (SMEs). Programs that have done extensive work in this area include Navy Joint Aviation Technical Data Integration, Navy Distance Support, Army Advanced Maintenance Aid Concept (AMAC), and SSC San Diego's Meteorology and Oceanography (METOC) Systems Knowledge Center.

Other programs that are promoting technologies for wireless and interactive information support include Navy Total Ship Monitoring, Navy Knowledge Projection, Air Force Xybernaut Wearable Computer Study, Department of Defense (DoD) Maintenance Mentoring System, and others. Currently, each is developing its own version of telemaintenance because of unique processes, organizational structure, and information requirements.

Many of these programs are already in development. As development matures, there is concern that duplicative software and tools will proliferate. Not only will these be costly to develop, train, and maintain separately, but separate development could drive processes and local data standards that will be counterproductive to supporting a joint force structure in a network-centric environment. In addition, the task of

creating this environment is enormous, and the cost is much greater than any one program can bear alone.

Because of these concerns, these programs have come together using the Joint Distance and Response (JDSR) Advanced Concept Technology Demonstration (ACTD) as a forum to share technology, infrastructure, and lessons learned. For example, through work conducted by SSC San Diego, plans are underway to have the Army AMAC system integrate with the Navy Knowledge Projection system to provide "intelligent" knowledge management. From a joint force command perspective, JDSR is leveraging the service programs to establish a common telemaintenance environment, and providing the integration to focus on timely employment of information to the maintainers. Together, a common robust telemaintenance system that has both a positive readiness and a positive cost impact to the services can be developed, tested, demonstrated, and deployed.

## OBJECTIVES

The objectives of the JDSR ACTD are to (1) increase the joint task force commander's warfighting equipment availability and readiness awareness with a reduced maintenance support footprint, mass, and inventory; (2) increase the service maintainers' efficiency; and (3) provide interoperable tool sets at the point of maintenance.

## CONCEPTUAL APPROACH

The *concept* is to project near-real-time national/global SMEs and knowledge to the warfighter/maintainer, as well as provide a platform to use telecommunication (collaboration, remote diagnostic support, help desk operation, condition/case-based maintenance, and interactive electronic technical manuals [TMs]). The result will be increased situational awareness of weapon systems and platform readiness for the joint task force commander. The *approach* is to integrate advanced commercial technologies with the services' ongoing development programs to provide a maintenance environment that is flexible, agile, and responsive to support the joint task force commander's needs, and to address the demanding challenges facing the military.

The *conceptual approach* uses telecommunication and the integration of technologies to focus on the timely employment of information/data (such as audio, video, technical, and logistics) to the different service maintainers under various deployed scenarios. JDSR will provide the combatant commanders/services with four integrated functions: remote collaboration, information/knowledge sharing, remote platform diagnostics, and distant training/maintenance mentoring. SSC San Diego has been researching various remote collaboration tools, including Collaborative Virtual Workspace (CVW), an open source collaboration tool.

Figure 1 shows the JDSR operational concept.

## DEMONSTRATION STRATEGY

The demonstration strategy is a three-step spiral demonstration process, culminating with a focused operational demonstration/joint military utility assessment (JMUA) to assess the JDSR technologies' capability to

enhance maintenance operations for the services. There will be three operational demonstrations; the final operational demonstration will be the JMUA. Technical demonstrations will precede each operational demonstration. The purpose of the technical demonstration is to obtain an initial functional interoperability and JMUA. During the operational demonstrations, the concept of operations/tactics-techniques-procedures will be validated and critical operational issues will be addressed, thereby achieving a credible JMUA. Figure 2 shows the JMUA technical demonstration strategy.

Operational Demonstration 1 will use an alpha system and demonstrate reachback capabilities of collaboration, remote diagnostic/prognostic support, web portal technologies, SME directories and support, transmission of imagery, and large files. Figure 3 shows the major elements of Operational Demonstration 1.

Operational Demonstration 2 will use a beta system and demonstrate the capabilities in Operational Demonstration 1, plus interactive support, mechanics compass, interoperability, data mining, and information dissemination. The services will be linked for information exchange relevant to ground, air, and sea equipment/systems, effectively attaining maintenance support at various levels. Figure 4 shows the major elements of Operational Demonstration 2.

JMUA/Operational Demonstration 3 will use a modified beta system and will demonstrate the capabilities in Operational Demonstration 2. It will also include lessons learned from Operational Demonstration 2. Operational Demonstration 3 will showcase the full JDSR capability

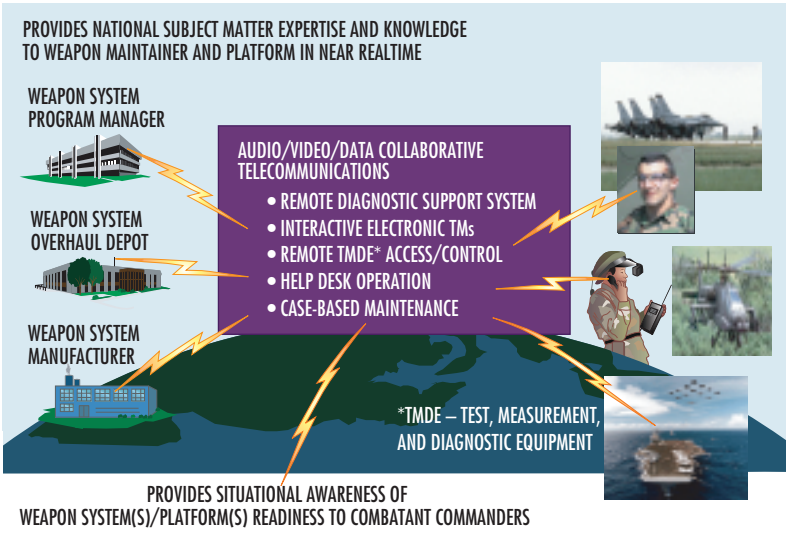


FIGURE 1. JDSR operational concept.

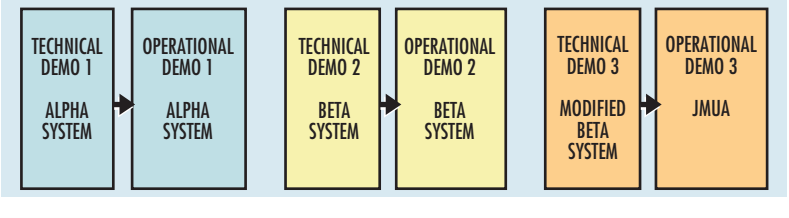


FIGURE 2. JMUA technical demonstration strategy.

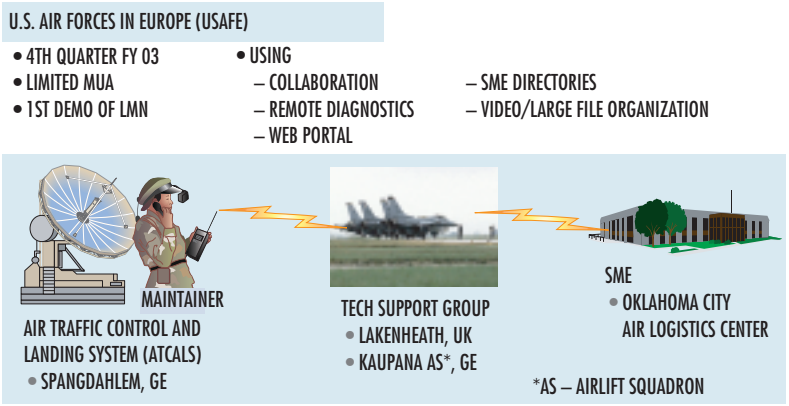


FIGURE 3. Operational Demonstration 1.

being employed for ground-, air- and sea-based platforms, as well as linking these platforms to maintainers, SMEs, repair depots, and industry experts. The objective is to demonstrate the end-to-end JDSR system and build on Operational Demonstration 2.

## TECHNICAL APPROACH

The implementation of the JDSR system consists of four key components: (1) the local maintenance network (LMN), consisting of the local-area network (both wired and wireless), the LMN server, and the LMN clients and their associated JDSR eTools software; (2) the communications network; (3) the distributed gateway; and (4) the support network. The goal is to provide near-real-time content and support to the maintainers by integrating and leveraging established distance support technologies and programs available from different DoD services. Figure 5 shows the JDSR architecture overview.

## CONCLUSION

To meet the warfighter/maintainer's requirements, the JDSR relies on leveraging other programs. JDSR leverages the armed services' telemaintenance programs, other advanced technology demonstrations, and industry independent research and development programs to create an integrated system usable across the services. JDSR uses existing infrastructure, COTS equipment, and software to augment the leveraged programs, creating a robust and secure environment that can support the services' unique maintenance processes and maintenance systems.

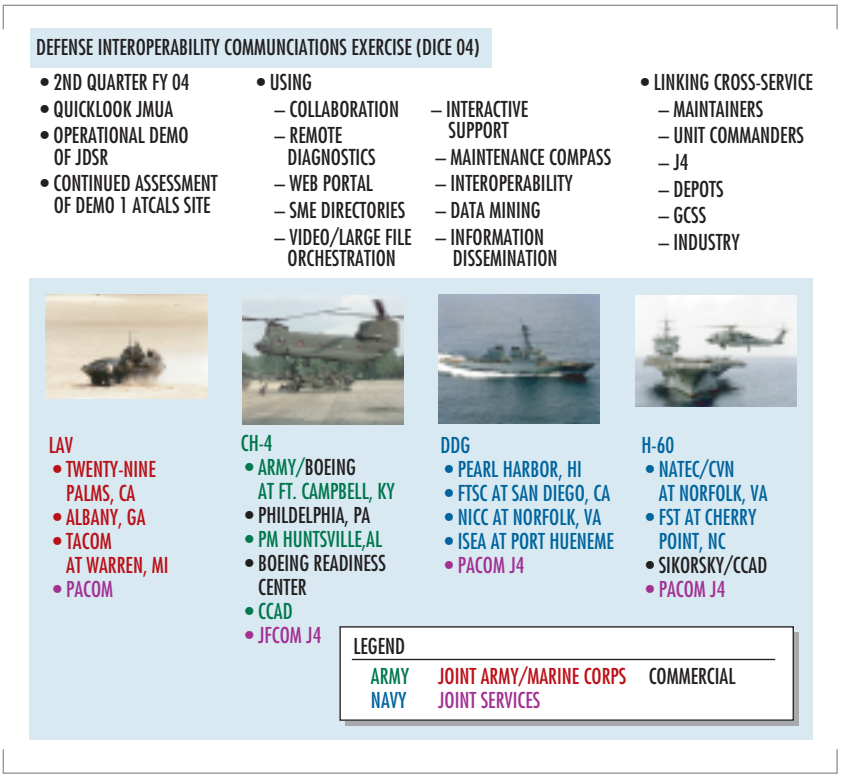


FIGURE 4. Operational Demonstration 2.

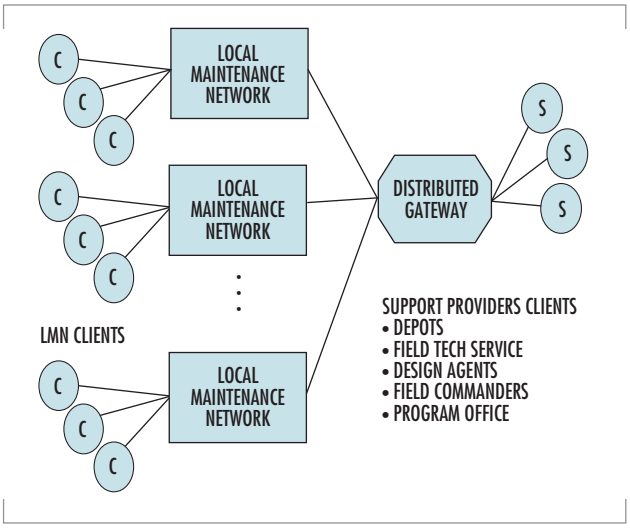


FIGURE 5. JDSR architecture overview.

**Ahn Nuzen**

BS, Computer Science, California State University at Chico, 1985

Current Research: Collaboration and communications interoperability architecture for JDSR ACTD.

**Bill Taw**

MBA, Indiana University, 1989

BS, Mechanical Engineer, Purdue University, 1972

Current Work: Technical Manager for JDSR ACTD.

# Advanced Technologies for Free-Space Optical Communications: Fiber Optic Beam Steering

**Michael Brininstool**
SSC San Diego

ABSTRACT

*Fiber optic beam steering (FOBS) offers unique features for free-space optical communication networks. FOBS devices can be employed on military platforms with constrained size, weight, and power limitations such as small, unmanned vehicles and individual warfighters. Compared to conventional beam control techniques, FOBS devices are significantly smaller and lighter and use no local power at the transmitter head. FOBS employs fiber Bragg gratings and, through selective mechanical or wavelength tuning, converts guided modes to radiation modes. This directional radiation can be delivered efficiently to free-space optical communications receivers. Three fundamental FOBS building blocks are described. Their performance features and trade-offs are summarized. Factors for improving radiation efficiency are discussed.*

## INTRODUCTION

Military systems are expanding in-theater communications capacity by employing the optical spectrum. Free-space optical (FSO) communications can bridge the merits of high-bandwidth fiber optics with flexible wireless networks. Building an agile optical-network layer helps alleviate radio frequency (RF) spectrum crowding. To enable connectivity between both fixed and mobile FSO nodes, precise and agile beam steering is paramount. Existing beam-steering approaches employ bulk optic techniques such as moving mirrors (gimbals or micro-electro-mechanical systems [MEMS]), prisms, liquid crystals, and/or Faraday phase retarders. While these systems offer high directivity, they can push the payload limits of size and weight for small platforms. Additionally, conventional steering techniques consume electrical power and require multiple heads to cover a 360-degree azimuthal field.

The author has devised several fiber optic beam-steering (FOBS) approaches. Bragg diffraction is used to direct a narrow beam of modulated light to a specified point in space. Conventional FSO beam controllers employ optical fiber simply as a conduit to transport the modulated carrier from the laser to the transmitter head. FOBS delivers agile beam control directly from a fiber element. This technology greatly simplifies the transition between the guided mode and radiated mode, enabling a seamless transition from laser source to atmosphere. Being all-optical, FOBS offers aperture heads with substantially reduced size and weight. No moving parts or electrical power are required. The FOBS technology form a unique class in terms of size, weight, and power requirements at the radiator head, but does so at a modest cost in directivity, bandwidth, and receiver complexity.

## THEORY OF OPERATION

Many beam-steering techniques employ diffraction gratings. The FOBS devices exploit features of fiber Bragg gratings (FBGs) that are common in optical telecommunications and sensors. FOBS devices are essentially optical phased arrays written into the core of an optical fiber. FOBS device operation is governed by the fundamental equation for Bragg diffraction of an incident fiber-guided mode:

$$m\lambda = d\,(1 + \sin\phi),$$

where m are the possible Bragg diffraction orders (m = 0, 1, 2, 3, …), λ is the wavelength of light in the fiber medium, d is the grating period of the index modulation written in the fiber core, and ϕ is the exit angle of the radiated mode as measured in the elevation plane, the plane parallel to the fiber axis (ϕ = 0 exits normal to the fiber axis).

The bulk of the work in the FBG field employs normal incident gratings, where the grating period is set to d = λ/2 (ϕ = 90°). These devices serve as narrow-band filters, reflectors, dispersion compensators, gain equalizers, and sensors. For normal-incident gratings, emphasis is placed on conserving the guided mode and thus minimizing radiative loss. In contrast, FOBS devices focus on efficiently converting guided modes to radiation modes. The Bragg diffraction equation shows that the radiation exit angle, ϕ, can be steered by tuning d or λ, within an operational region at 1550 nm of $0.6 < d/\lambda < 1.2$. Within this range, only the first diffraction order (m = 1) provides radiation from the core. Tuning of d can be accomplished by fiber strain. Changing λ can be done by direct tuning of the transmitter wavelength. Radiated beam patterns along the elevation plane are transforms of the grating array function. Depending on the optical linewidth of the source and the length of the grating, FOBS devices can be designed to be diffraction-limited to narrow divergence ($10^{-3}$ degrees) or filled to patterns covering 20 degrees. In azimuth (the plane normal to the fiber axis), the radiation pattern is the transform of the grating element function.

## FOBS BUILDING BLOCKS

### Broadbeam Optical Aperture (BOA)

Once the fundamental building blocks have been demonstrated, many FOBS device configurations can be realized. At the heart of all configurations is the broadbeam optical aperture (BOA). The BOA consists of a single optical fiber. For purposes of discussion, we start with the BOA mounted vertically. An FBG is written perpendicular to the fiber axis and the grating spacing is set between $0.7 < d/\lambda < 0.9$. As shown in Figure 1, the BOA emits a full, 360-degree beam in azimuth. The center of the elevation angle depends on the choice of d/λ. The elevation divergence is very narrow, and its pattern is determined by the grating array function and dispersion. For a 20-mm-long grating, the elevation divergence is only about $3 \times 10^{-3}$ degrees. At these beam widths, the transmitter head gain or directivity (defined relative to an isotropic radiator) is 45 dB. The elevation plane of the exiting beam can be steered by using strain or wavelength tuning over a practical range of ±5 degrees. To first order, the bandwidth of the BOA can be estimated from the time delay of a pulse traversing the entire grating length. The bandwidth of the BOA decreases linearly with increasing length. For example, the bandwidth of a 20-mm aperture is about 3.5 GHz. These facts illustrate the classic gain-bandwidth trade-off. Since radiation efficiency and directivity from the FOBS device increase with increasing grating length, higher radiation efficiency and directivity mean lower bandwidth.

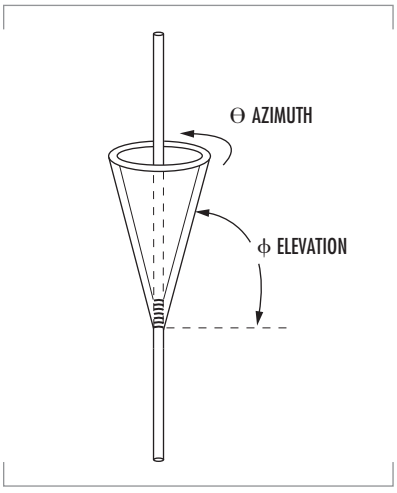


FIGURE 1. Radiation pattern for BOA device with full azimuthal coverage.

### Vertically Indexed Power-Efficient Radiator (VIPER)

Directivity of the BOA can be sharply improved by tilting or blazing the grating away from normal incidence. Blazing the grating increases directivity by concentrating the radiation into a narrow, element-function

dependent beam, as shown in Figure 2. For a blazed BOA, the azimuthal divergence is determined by the element function of the grating array, as depicted in Figure 3. Once the radiation angle is chosen, an optimum blaze angle inside the core can be written. Blazed gratings suffer from polarization fading. It is the interaction between the incident guided mode and the blaze that determines the Transverse Electric/Transverse Magnetic (TE/TM) mode ratio, or fade. In theory, a blaze at 45 degrees relative to the incident mode (optimum for a 0-degree exit angle) results in infinite polarization-induced fading. In practice, for 5-mm gratings and an estimated index perturbation of $5 \times 10^{-4}$, fades of 25 dB were measured. To first order, for a planar, disk-shaped, 10-mm array element, the azimuthal beam full width to the first set of nulls (Figure 3) is found from diffraction to be approximately 10 degrees. Compared to an unblazed BOA, blazing gives 15 dB of directivity improvement for a total of 60 dB. Directivity enhancements from blazing are traded for increased complexity in the FOBS configuration. To implement azimuthal beam steering around the full 360-degree field of regard, at least 36 blazed BOA devices would have to be arranged vertically in a circular array, called a VIPER (vertically indexed power-efficient radiator). Azimuthal beam steering can be performed by selectively activating a specific sector fiber with an optical fiber switch. VIPERs have the same bandwidth characteristics as BOAs but have higher directivity. Higher directivity can, in turn, enable a longer communications range between nodes or a higher bandwidth at the receiver.

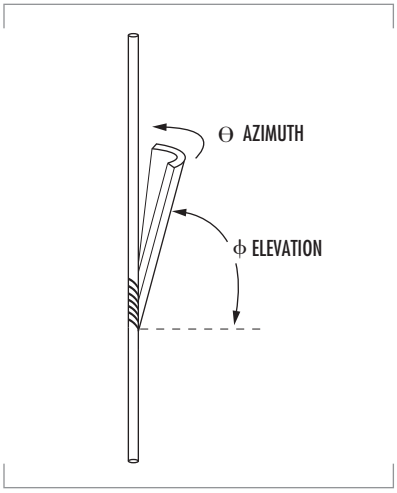


FIGURE 2. Improved beam directivity in azimuth for blazed BOA.

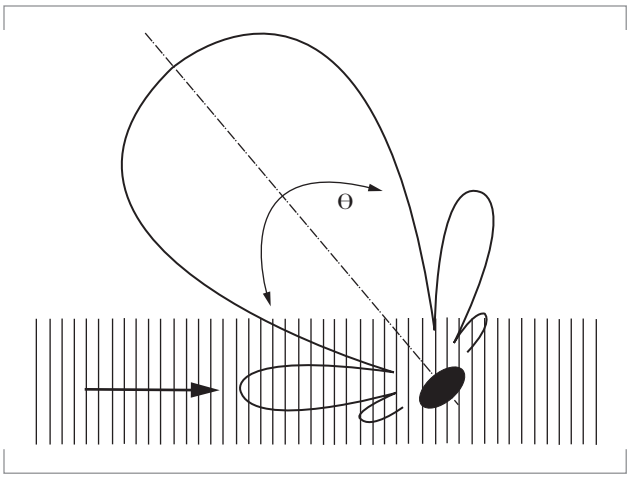


FIGURE 3. Grating element function determines shape of radiated azimuthal beam pattern for blazed BOA.

### Coiled Optical Broadbeam Radiating Aperture (COBRA)

A set of blazed FBGs could be written onto a coil of fiber called a COBRA (coiled optical broadbeam radiating aperture). If oriented horizontally, each FBG would be dedicated to a defined azimuthal sector, as shown in Figure 4. In this configuration, radiation divergence in elevation is now set to the element function (less than 10 degrees), and the beam can be steered within each azimuthal sector by tuning grating period or wavelength. Directivity, efficiency, and bandwidth are sacrificed for the sake of providing full azimuthal coverage and tuning. Since directivity is low (roughly 25 dB), it is envisioned that COBRAs would be most useful as FSO beacons for the point, acquisition, and track (PAT) subsystem. The COBRA could transmit relative heading information encoded as a unique wavelength that is decoded at the receiver. This technique is particularly easy to implement for receivers in coherent systems. The receiver's local oscillator could track the sweeping COBRA wavelength and extract the relative bearing of the transmitter. COBRA fabrication poses several challenges. The writing beams would have to be aligned in the same plane as the exit radiation, a difficult task for blazed gratings. Also, it would be preferable to write the gratings on the coiled surface instead of incurring alignment errors by coiling the fiber after grating formation. Coiled grating production would likely require a specialized phase mask, most probably a flexible holographic optical element (HOE).

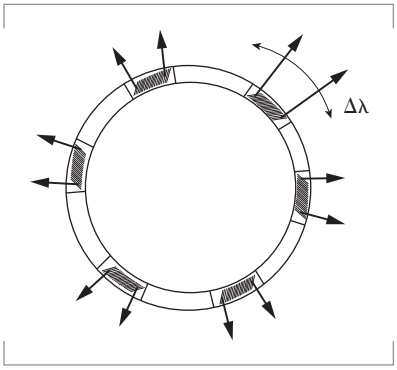


FIGURE 4. Blazed fiber Bragg gratings are assigned azimuthal sectors in COBRA design.

## FOBS PERFORMANCE

Work performed at SSC San Diego on blazed fiber Bragg gratings has led to establishing baseline performance milestones. In Table 1, the results from preliminary analyses reveal a range of device performance expectations. The values shown in the table are for calculations with a radiation-unit-efficiency range chosen to be from 1 to 10%/mm.

TABLE 1. Performance comparison summary for FOBS building blocks.

| Device Characteristic | BOA | VIPER | COBRA |
|---|---|---|---|
| Bandwidth per beam | 30 MHz to 3.5 GHz | 30 MHz to 3.5 GHz | 1 to 200 MHz |
| Directivity | 55 to 45 dB | 70 to 60 dB | 45 to 25 dB |
| Azimuthal Coverage | Fixed Full 360° | Steerable Full 360° | Steerable Full 360° |
| Elevation Coverage | Steerable ± 5° | Steerable ± 5° | Fixed ± 5° |
| Size (radius x height) | 0.10 mm x 225 to 20 mm | 1.4 mm x 225 to 20 mm | 50 mm x 65 to 0.25 mm |

Demonstrations show radiation-unit efficiencies of about 1%/mm. The challenge for transition to useful FOBS devices is to improve the efficiency of radiative FBGs, for both normal incidence and blazed designs. Induced current models similar to those employed in antenna theory have been developed to predict coupling between bound and radiation modes [1 and 2]. The models view the grating as a continuous distribution of radiating dipoles driven by an incident-bound fiber mode. The grating is, in essence, a linear optical phased array made from a set of thin dielectric mirrors. The models and subsequent laboratory demonstrations validate that radiation efficiency increases linearly with grating length but grows with the square of the refractive index modulation depth. High index modulation depends on many factors: source wavelength and coherence, exposure time and fluence, fiber dopant concentration, fiber index profile, fringe visibility in fiber core, suppression of zero-order diffraction from the phase generator, and environmental vibrations. The success of FOBS relies on employing fiber with high photosensitivity. To obtain enhanced photosensitivity, fibers designed especially for grating production use co-dopants. Hydrogen-loaded fibers with B/Ge, Ge/Yb, and Ge/Tm co-dopants are good candidates for improving index modulations up to $10^{-2}$ [3].

Performance issues impact fabrication trades for blazed FBGs. Several facts have emerged from blazed FBG modeling, fabrication, and characterization performed at SSC San Diego. As the exit angle is increased away from zero (normal to the fiber axis and $d = \lambda$) and moved farther into either the backward- or forward-scattered direction, many things improve: radiation efficiency increases, polarization fade decreases, elevation-beam divergence decreases, and wavelength-tuning slope efficiency increases. All of these facts suggest production of gratings with high exit angles. The disadvantage to high exit angles is increased beam distortion encountered as the light escapes the cylindrical cladding–air boundary. This distortion has yet to be modeled. Also, for vertically mounted BOA and VIPER systems, a higher exit angle limits the horizontal range flexibility for an orbiting node's receiver. Limits on turning radii at operational speeds for orbiting communications platforms coupled

with requirements for system bandwidth and head directivity will ultimately bound the practical upper limit for exit angles.

The FOBS devices are best suited for supervisory, broadcast applications where the radiator serves to deliver high-bandwidth data to numerous fixed and mobile nodes. For fixed-node dissemination, each subservient receiver node could be assigned a specific wavelength address corresponding to unique spatial coordinates relative to the radiator. For mobile applications, orbiting nodes would be assigned range and altitude corresponding to unique orbits, thereby minimizing the need to shift wavelengths in order to track the nodes' position. The BOA simply radiates in full azimuth and sets an elevation ring based on wavelength. The VIPER gives higher directivity, better azimuthal steering control, but at the expense of production complexity. In many instances, it is the orbiting node that has data to download to the supervisor. In these applications, broadband modulating retro reflectors (MRRs) could be mounted onto the mobile platforms to impress data onto continuous-wave (CW) carriers emitted from the FOBS node.

## CONCLUSION

As FSO technologies continue to advance, the subset of beam-steering technologies will emerge with definable trade-space coordinates. These trades will be based on mission, platform, and cost parameters. FOBS devices promise to fill unique niches within those trade spaces. Special focus will be on applications requiring multi-wavelength simultaneous broadcast and for platforms with constrained size, weight, and power limits such as mobile, unmanned vehicles, buoys, and disadvantaged warfighters. Future work will emphasize enhancing grating radiation efficiency and performing detailed trades in order to transition the fundamental FOBS building blocks into useful systems. This work will be expanded to include beam-steering techniques that use gratings made in planar optical waveguides. Higher radiation efficiency is gained at the expense of fabrication complexity, mode-field mismatch loss, and reduced flexibility in building circularly symmetric components.

## ACKNOWLEDGMENTS

This work was performed with funds from SSC San Diego's Science & Technology Capabilities Initiatives Program and the Defense Advanced Research Projects Agency (DARPA) Advanced Technology Office (ATO) Tera Hertz Operational Reachback (THOR) program. The author thanks Joseph Aboumrad, John Boyd, Steven Cowen, Chris Csanadi, Douglass Evans, Earl Floren, Justin Hodiak, Joseph Morales, Susan Morales, Po Tang, and Ronald Tong for their valuable contributions to the modeling, fabrication, and characterization of fiber Bragg gratings.

REFERENCES

1. Snyder, A. W. and J. D. Love. 1983. *Optical Waveguide Theory*, Chapman Hall, New York, chap. 21.
2. Meltz, G., W. W. Morey, and W. H. Glenn. 1989. "Formation of Bragg Gratings in Optical Fibers by a Transverse Holographic Method," *Optical Letters*, vol. 14, pp. 823–825.

3. Campbell, R. J. and R. Kashyap. 1994."The Properties and Applications of Photosensitive Germanosilicate Fibre," *International Journal of Optoelectronics*, vol. 9, p. 33.



**Michael Brininstool**

BS, Electrical Engineering, Arizona State University, 1980

Current Research: Free-space optical communications; undersea optical communications.

# The Rough Evaporation Duct (RED) Experiment: Microwave and Electro-Optical Transmission Experiments in the Air–Sea Boundary Layer

**Kenneth D. Anderson, Stephen M. Doss-Hammel, and Richard A. Paulus**
SSC San Diego

ABSTRACT

*Microwave and electro-optical (EO) signal propagation over a wind-roughened sea depends on signal interaction with the sea surface and the vertical profiles of pressure, temperature, humidity, and wind. Yet, within the marine surface layer, these mechanisms are not sufficiently understood. To address this deficiency, the Rough Evaporation Duct (RED) experiment was designed to provide data for validation of meteorological, microwave, and EO models in the marine surface layer for rough surface conditions, including the effects of surface waves. The RED experiment was conducted offshore the Hawaiian Island of Oahu in late summer, mid-August to mid-September, of 2001. Led by SSC San Diego and sponsored by the Office of Naval Research, the RED experiment was designed to assess the effects of the air–sea boundary layer on naval radar and EO systems performance in detecting high-speed, low-flying sea-skimmer missiles.*

## INTRODUCTION

When radars first came into operation during the late 1930s, they were not expected to detect targets much beyond the geometrical horizon. Operating at a wavelength of 13 m, these early radars generally met expectations. As new radars were rapidly developed, operating at shorter and shorter wavelengths, the shorter the wavelength the more frequent were observations of unorthodox, or anomalous, propagation effects. For example, when 10-cm radars were installed along the south coast of England, they were often able to see the coast of France, well beyond the geometric horizon. These anomalous propagation effects also became more pronounced as the radar's operating area became more tropical. By the end of World War II, it was clear that meteorological conditions in the lowest portion of the atmosphere, the troposphere, could be used to describe qualitatively, sometimes quantitatively, the observed anomalous propagation effects.

During World War II, A. S. Monin described the vertical distribution of meteorological quantities within the tropospheric surface layer (extending tens of meters vertically from the interface between the earth's surface and the troposphere). In the late 1960s, Monin-Obukhov Similarity (MOS) theory was experimentally confirmed over land and adapted to model microwave propagation over the sea. Experimental work in the late 1960s and early 1970s clearly identified a persistent meteorological phenomenon capable of confining, or ducting, microwave signals within the surface layer and propagating these signals to ranges well beyond the radio horizon. This meteorological phenomenon is called an evaporation duct because it is related to the rapid decrease in water vapor in the first few meters above the sea surface.

Significant advances in computational capabilities beginning in the early 1970s allowed relatively rapid and extensive calculations of RF propagation, which led to the development of the first operational propagation assessment system, the Integrated Refractive Effects Prediction System. By the end of the 1980s, computational capabilities for propagation assessment had made even greater strides; models developed include a rigorous solution for conditions of meteorologically horizontal stratification and an approximate solution where meteorological conditions change with range. With extensive development over the years, including capabilities to assess land effects and surface roughness, these new models have been incorporated in the latest operational propagation assessment system, the Advanced Refractive Effects Prediction System (AREPS).

Much of the development of infrared sensing systems was driven by military needs in the twentieth century. In particular, the development of heat-seeking infrared-guided missiles such as the Sidewinder drove development of improved infrared detectors and better infrared (IR) propagation models. Shipboard infrared search and track systems (IRST) offer a passive detection capability and excellent angular resolution, and they can be used to complement radar systems. The continuing development of increasingly sensitive detectors, including imaging infrared systems, and better optical components, has helped to spur the development of IRST systems.

We present results from a recent set of experimental measurements relating to microwave and IR propagation over the sea. The following sections briefly review the experiment setup and modeling, discuss the significant results for both RF and infrared propagation, and provide a summary.

## EXPERIMENT SETUP AND MODELING

Figure 1 illustrates the geometry of the RED experiment. The research platform Floating Instrument Platform (R/P *FLIP*), shown in Figure 2, was three-point moored in about 300 m of water with its keel aligned into trade winds that were typically from 080° at about 5 $ms^{-1}$. Its port boom, extending about 17 m from the hull in a northerly direction (see Figure 2), was fitted with a vertical mast that was instrumented with the sensors described in Table 1. Additional meteorological (met) sensors were located on a "flux-buoy," positioned midway between R/P *FLIP* and shore along the 10-km EO path, and on a "mean-met" buoy positioned midway on the 25.7-km RF path. Two sets of three continuous wave (CW) microwave transmitters were installed on the starboard side of R/P *FLIP*, and the receiver site was located at the Marine Corps Base Hawaii. From this site there was an unobstructed view to the transmitters located on R/P *FLIP*. Each transmitter was sampled sequentially in time at a 1-Hz rate for 256 seconds. The sequencing started at the hour and half-hour, beginning with the high antenna and then switching to the low antenna; the bands were sampled in order of Ku, X, and then S. For the current work, the received signal levels were calibrated to propagation loss and then averaged into 5-minute intervals.

IR measurements were collected by a transmissometer system, consisting of a broad-beam transmitting source and a receiving telescope. The source used 18 halogen lamps, modulated by a 690-Hz chopper wheel, and had a usable beam width of approximately 25°. The chopper signal was relayed to the receiver via a radio link at 162.1 MHz, where it was used to phase-lock a signal amplifier. Figure 2 shows the location of the IR source onboard R/P *FLIP*. The receiver telescope's primary mirror was a gold-plated

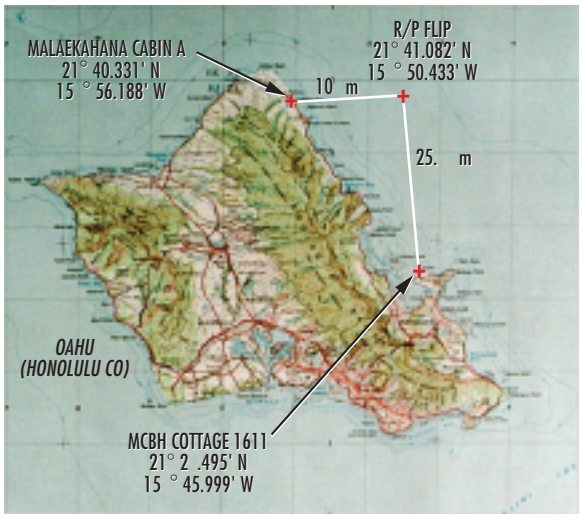


FIGURE 1. The geometry of the RED experiment.

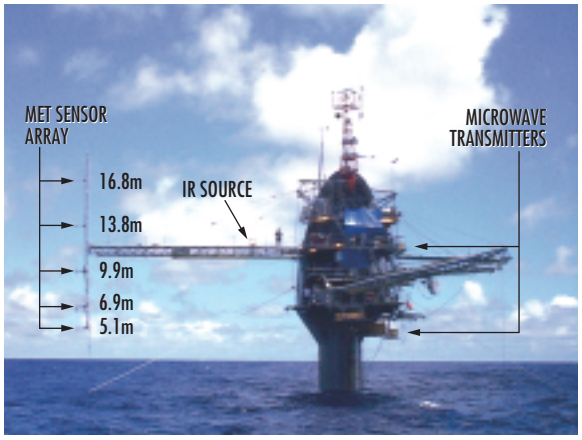


FIGURE 2. R/P *FLIP* as moored for RED.

parabolic 20 cm in diameter with a focal length of 1.22 m, yielding an F ratio of 6. The mid-wave detector, a non-imaging device cooled to 77°K, was a 2-mm-diameter InSb photodiode mounted below a cold optical filter with an almost square bandpass between 3.5 mm and 4.1 mm. For a given source radiance, the detector responsivity, noise density, and bandwidth determine the signal-to-noise ratio. For the transmission measurements, the lock-in time constant was set to 3 seconds, and the data were sampled once per minute. Higher speed scintillation measurements were made every 15 minutes, where the lock-in time constant was set to 1 ms and the data sampled at a 300-Hz rate for 109 seconds.

TABLE 1. The met sensors installed by the University of California, Irvine (UCI) on the vertical array. (A) mean wind speed and direction, (C) and (G) three-dimensional (3-D) mean and turbulent wind and temperature, (D) mean specific humidity, (H) mean temperature, (K) and (L) mean and turbulent specific humidity, (S) sea-surface elevation.

| Level | ASL (m) | Sensor |
|---|---|---|
| -1 | 0.0 | S,H |
| 0 | 3.1 | G |
| 1 | 5.1 | C,L,D,H |
| 2 | 6.9 | C,L,D,H |
| 3 | 9.9 | C,L,D,H |
| 4 | 13.8 | C,K,D,H |
| 5 | 16.8 | G,D,H |
| 6 | 19.8 | A |

| | |
|---|---|
| A | Cup & Vane |
| C | Campbell CSAT3 Sonic |
| D | EdgeTech Dew Pointer |
| G | Gill Sonic |
| H | Hart Thermistor |
| K | Campbell Krypton Hygrometer |
| L | MM Lyman-Alpha Hygrometer |
| S | SIO Wavewire |

## OBSERVED AND MODELED PROPAGATION EFFECTS

Figure 3 illustrates the comparison of observed and modeled propagation loss for the high-sited and low-sited X-band links during the RED experiment. The reference lines labeled "free space" correspond to the propagation loss expected if the link paths were in free space, that is, a vacuum with no obstructions between the transmitters and receiver. The reference lines labeled "standard atmosphere" correspond to the propagation loss expected for atmospheric conditions of a well-mixed, or standard, troposphere. The observed signal levels (blue dots) are consistently near free space for the high transmitter and nearly always exceed free-space levels for the low transmitter. The mean and standard deviation of the difference between the observed and modeled (red crosses) propagation loss is –0.17 and 4.01 dB for the high-sited transmitter and 4.27 and 3.44 dB for the low-sited transmitter. The modeled data for this example were derived using the meteorological data collected by University of California, Irvine (UCI) at level 1 on the vertical array with the Naval Postgraduate School (NPS) bulk model using Businger–Dyer profile functions of T and Q.

Table 2 lists the minimum, maximum, mean, and standard deviation of the difference between the observed and calculated propagation loss for models, geometries, and frequencies described above. Results from using other sources of the meteorology, such as the flux-buoy or different levels from the UCI array, gave similar differences between the observed and modeled propagation loss. Considering the mean and standard deviation, all models are essentially equally good predictors.

For IR transmission, signal extinction due to aerosols and gases was a significant effect. The model for extinction was generated in a two-step process. First, MODTRAN (Moderate Resolution Transmittance Code) was used to predict gaseous

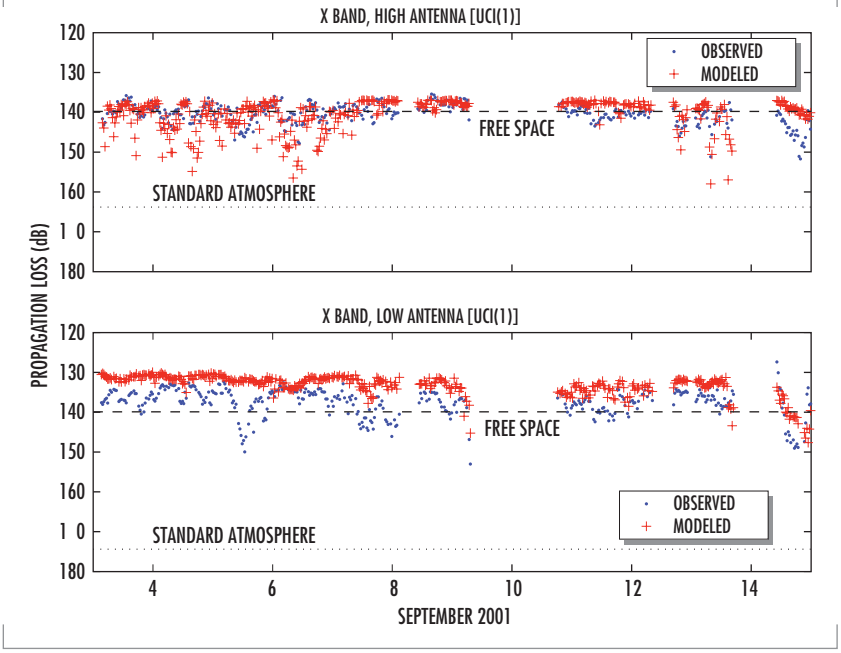


FIGURE 3. Comparison of modeled (red crosses) to measured (blue dots) propagation loss for both the high- and low-sited X-band (9.6 GHz) transmitters during RED. The modeled data are derived from meteorological measurements at level 1 (5.1 m asl) of the UCI array.

extinction for each meteorological data point. The second step of the process used the Advanced Navy Aerosol Model (ANAM) to predict the effects of aerosols on propagated signals. The ANAM model extends and elaborates the single-height Navy Aerosol Model (NAM) model by providing a height-dependent extinction profile. In addition to ANAM, signal extinction was calculated from data provided by optical aerosol classifiers that were mounted on R/P *FLIP*. Figure 4 shows the comparison of modeled to observed IR transmittance for a 3-day period. Day 251 corresponds to 8 September 2001. The green line, at a transmittance of about 0.3, is the molecular transmittance calculated by MODTRAN; the red and blue lines are the product of aerosol and molecular extinction (giving the total calculated transmittance) for the observed aerosol distribution and for the modeled aerosol distribution derived from ANAM, respectively. The black line, corresponding to the observed transmittance, is 40% to 65% of the calculated transmittance. The reason for this discrepancy between modeled and observed transmittance has not yet been resolved. Possible explanations are additional aerosol extinction from the surf zone or aerosol loading by organics. Investigation of these and other possible explanations is ongoing.

TABLE 2. The mean, standard deviation, maximum, and minimum difference between the observed and calculated propagation loss (dB) for the three frequency bands (S is 3.0 GHz, X is 9.7 GHz, and Ku is 17.7 GHz) and the two transmitter heights (high is ~13 m asl and low is ~5 m asl). The calculated propagation loss was computed using NPS "bulk model" (TOGA-COARE form) with meteorological inputs from level 1 (5.1 m asl) of the UCI array.

| | High Transmit Antenna | | | | Low Transmit Antenna | | | |
|---|---|---|---|---|---|---|---|---|
| | Mean | Std | Max | Min | Mean | Std | Max | Min |
| S-Band | 2.69 | 2.31 | 9.53 | -4.77 | 2.84 | 2.15 | 15.12 | -3.10 |
| X-Band | -0.17 | 4.01 | 11.24 | -16.09 | 4.27 | 3.44 | 18.63 | -13.79 |
| Ku-Band | 2.68 | 5.82 | 18.87 | -14.77 | 5.40 | 7.39 | 21.64 | -18.92 |

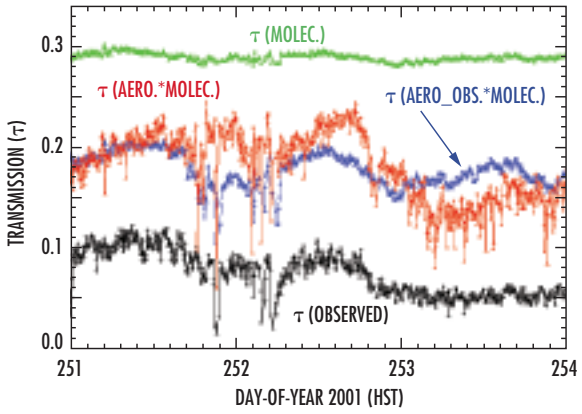


FIGURE 4. Comparison of modeled (red and blue lines) to measured (black line) IR transmttance for day-of-year 251 to 254 (8–11 September 2001).

## SUMMARY

The RED experiment was conducted off the Hawaiian Island of Oahu in late summer, mid-August to mid-September of 2001. In addition to R/P *FLIP*, two land sites were instrumented with microwave and EO receivers and meteorological sensors, two buoys were deployed, a small boat was instrumented, and two aircraft flew various tracks to sense both sea and atmospheric conditions. Eleven scientists and engineers were aboard R/P *FLIP* and installed instruments measuring mean and turbulent meteorological quantities, sea wave heights, flow direction, wave kinematics, upward and downward radiance, near surface-bubble generation, atmospheric particle size distributions, laser probing of the atmosphere, and sources for both microwave and electro-optic signals. In all, more than 25 people from four countries, six universities, and four government agencies were directly involved with the RED experiment.

The major accomplishments of the RED experiment are:

- RED RF data analysis confirms that Monin-Obukhov Similarity Theory combined with a high-fidelity propagation model is a very good predictor of RF propagation in a homogeneous unstable marine

boundary layer. This leads to a high confidence in the AREPS operational propagation assessment system.

- RF, EO, and meteorological data collected during RED provide a high-quality benchmark data set that will be useful for validation of new models (e.g., a periodic refractivity profile in both range and height).
- RED confirmed observations made during the 1996 Marine Boundary Layer experiment that height variations in scalars (air temperature, humidity, etc.) are related to sea waves and supports Miles' critical layer theory.
- RED provided the first direct evidence that the specific humidity profile function over the sea is not equivalent to the heat profile function (results from Coupled Boundary Layers/Air–Sea Transport may confirm this observation).
- RED demonstrated that organics are an important factor in aerosol scattering as aerosol hygroscopicity is lower than expected from inorganic sea salt alone, and speciated organics significantly contributed to the aerosol mass.
- RED showed that mid-wave infrared signals propagate poorly near the ocean surface in a windy, tropical environment, and that the signal deficit is under-predicted by current models.

**Kenneth D. Anderson**
BS, Electrical Engineering, San Diego State University, 1972

Current Research: Air–sea boundary layer effects on microwave propagation; sensors for characterizing wind, temperature, humidity, and pressure turbulence; Global Positioning System (GPS) sensing of tropospheric refractivity.

**Stephen M. Doss-Hammel**
Ph.D., Applied Mathematics, University of Arizona, 1986

Current Research: Propagation of visible and infrared signals in the marine atmospheric surface layer; effects of mirages and turbulence on signal propagation.

**Richard A. Paulus**
MS, Meteorology and Oceanography, Naval Postgraduate School, 1978

Current Research: Visibility in the littoral for characterization of aerosols; scattering for high-energy laser propagation.

# Expeditionary C5 Grid (EC5G) FY 02 Limited Objective Experiment

**Daniel E. Cunningham, Ayax D. Ramirez, Kenneth Boyd, Norman E. Heuss, and James Mathis**
SSC San Diego

ABSTRACT

***The Expeditionary Command, Control, Communications, Computer, Combat System Grid (EC5G) project is working to transform network-centric warfare concepts into operational practice. EC5G's primary effort for fiscal year (FY) 02 was a laboratory-based limited objective experiment (LOE) designed to investigate FY 06-07 mission capability enhancement using a global Internet Protocol (IP) architecture design that integrated a tactical shore backbone with satellite communications (SATCOM), line-of-sight, and information security. The approach was a comprehensive set of IP networking experiments conducted on a laboratory architecture built to model key components of a mini-fleet network. LOE accomplishments included designing and validating a layered network architecture that enables seamless worldwide mobility for naval forces, validating the value of such a network for the seamless transport of time-critical targeting data, validating quality-of-service designs and policies that distribute traffic over multiple SATCOM paths and prioritized traffic on a congested network, validating strategies for IP to the cockpit and ship-to-ship line-of-sight/beyond line-of-sight networking, and validating mechanisms for ad-hoc, any-to-any connectivity for security enclaves.***

## INTRODUCTION

The Expeditionary Command, Control, Communication, Computer, Combat System Grid (EC5G) initiative is the information transport cornerstone of the Navy's FORCEnet initiative. With a focus on time-critical strike and warfare capability improvement, EC5G is part of the U.S. Navy's effort to rapidly field a fully netted, global, adaptive, secure Internet protocol (IP) network for the naval and joint forces. EC5G is embarked on a multi-year process of experimentation; rapid prototyping; tactics, techniques, and procedures development; and program of record transition. Key collaborators for the limited objective experiment (LOE) described here included the Advanced Deployable System (ADS) program and the Office of Naval Research's (ONR's) Fleet Enterprise Network (FleetNet) Project, part of the Knowledge Superiority and Assurance Future Naval Capability (KSA FNC) program.

EC5G's primary effort for FY 02 was a laboratory-based LOE designed to investigate the 2007 capability potential of a global IP network and security architecture. The LOE hypothesis was that warfighting effectiveness could benefit from a converged IP network featuring end-to-end, global IP quality-of-service (QoS) support for high-priority, tactical traffic. The design objective was a global routing model that could naturally stem from and leverage the Navy's investment in Cisco routing technology that the ADNS program is installing on ship and shore nodes. The QoS design objective was end-to-end support for priority IP traffic and multiple security enclaves sharing the same network over KG-175 (FASTLANE® or TACLANE) IP-encryption devices.

## LOE OVERVIEW

The LOE consisted of a comprehensive set of IP networking experiments conducted on a laboratory architecture built to model key components of a global force network. The LOE network was designed to resemble a scaled-fleet network (Figure 1), including three shore nodes, six ship nodes, two aircraft nodes, three military satellite communication links to each ship, two Joint Tactical Radio System (JTRS) line-of-sight (LOS) networks, a beyond line-of-sight (BLOS) network relay, tactical communications data link (TCDL) point-to-point links from ship and air nodes, and three independent network security domains. Specific hardware included 45 Cisco routers, 20 Cisco switches, 65 PCs, 2 SATCOM

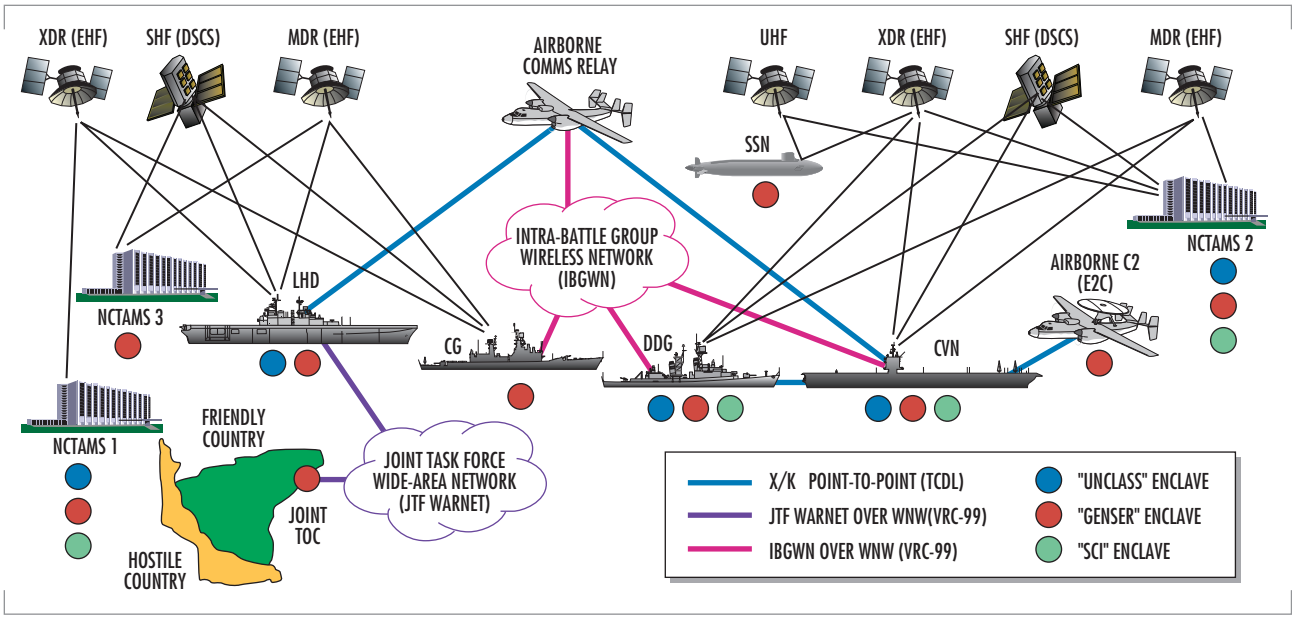


FIGURE 1. The EC5G LOE built a laboratory model of a next-generation global IP network for the Fleet. The LOE investigated technical integration issues as well as operational value brought to the warfighter.

simulators, 12 TACLANEs, 8 VRC-99 radios, and 2 programmable advanced transmission) multiplexers. The LOE network was distributed between five laboratory locations at SSC San Diego, connected seamlessly via virtual local-area networks over fiber.

Individual network experiments were designed as sub-tests to investigate specific network performance concerns. The 11 focus areas were:

1. Prioritized Network Traffic – guaranteeing network capacity in presence of congestion.
2. Latency-Bound Delivery Service – for high-priority service.
3. Load Distribution – to fully use every available link off a platform.
4. Ship-to-Ship LOS and BLOS Networking – for seamless QoS.
5. Airborne IP Services – to provide high-capacity Secret Internet Protocol Router Network (SIPRNET) to aircraft nodes.
6. Global Information Transfer (Network Operations Center [NOC]-to-NOC) – for transfer of time-critical strike data.
7. IP Network Encryption – to support global domains and policies.
8. Embedded Firewalls – for Layer 3 security access and control.
9. SATCOM Crosslink – to investigate inter-area of responsibility (AOR) routing and information assurance.
10. Joint IP Connectivity – to show integrated IP routing between Navy and joint nets.
11. End-to-End Scenario – to exercise global QoS policy and architecture.

Network routing and QoS architectures, operational scenarios, measures of effectiveness (MOEs), measures of performance (MOPs), and data collection approaches were designed to support the 11 focus area experiments.

## NETWORK DESIGN

The current afloat network is based on single or multiple routing domains per AOR. Per AOR routing means that direct network discovery and communications cannot be provided between ships or shore resources in different AORs. EC5G implemented a layered, global routing architecture using enhanced interior gateway routing protocol (EIGRP) and a single autonomous system for all general service (GENSER) network routers. A routing hierarchy design was implemented that includes three layers. The "core" network layer includes the NOC routers that receive all routing updates and know all SATCOM routes to every ship. The "media" layer includes shore routers that route traffic from a core router through a particular SATCOM system. A media router is only aware of nodes attached to that SATCOM system. The "ship" layer routers are responsible for routing all IP traffic (via SATCOM or LOS) on and off of the ship. This layered routing approach enabled implementation of a single global Navy routing domain while maintaining minimum routing updates to ships. Minimizing routing updates to ships provides optimized network convergence, reduces route traffic overhead, and simplifies network management.

## OPERATIONAL SCENARIO

The LOE scenario featured a rapid deployment of two battle groups (BGs) from different AORs. The BGs conducted initial planning for the battle enroute, conducted time-critical strike missions in theater, and operated together while communicating via different naval computer and telecommunications area master station (NCTAMS) and LOS links. The ships worked seamlessly and automatically through the global net as they moved around the world conducting network-centric warfare. For the Focus Area 1 experiments, for example, the CVN (aircraft carrier, nuclear) communicated with NCTAMS2 and switched between a combination of three different satellite resources at different times, providing guaranteed minimum capacity for several classes of marked IP traffic types (Figure 2).

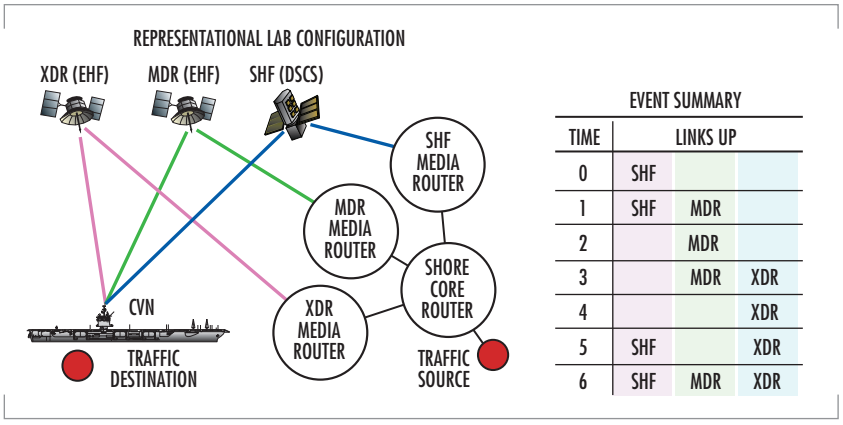


FIGURE 2. The LOE Focus Area 1 investigated priority-based routing of IP traffic over multiple SATCOM links to a ship.

## DATA COLLECTION AND ANALYSIS

Experimental data were collected using Chariot, a tool that emulates network users by sending traffic over the network; PacketShaper®, a tool that identifies traffic on the network at a localized node; and Cisco Quality of Service Device Manager (QDM), a browser-based application that runs from Java™. QDM is used to monitor and configure IP-based QoS functionality within Cisco routers. The combination of these three tools facilitated the development of scenario-based MOEs and MOPs for

assessing the ability of the network to support warfighting needs. Specific metrics included throughput samples, response time, one-way-delay, and transaction rate samples using the Chariot tool; traffic bandwidth by type and channel-utilization statistics using the PacketShaper tool; and traffic rate per QoS class using the QDM tool.

## EXPERIMENTAL RESULTS

One of the Focus Area 1 (prioritized network traffic) experiments is well suited for conveying a flavor of the LOE. The objective of this experiment was to guarantee a minimum, seamless capacity for high-priority IP traffic on a congested, dynamic, multi-link network. The scenario tested the network's ability to provide traffic prioritization, distribution, and fail-safe redundancy using multiple radio frequency (RF) satellite links during communications between NCTAMS2 and the CVN.

The Focus Area 1 experiment focused on IP traffic flow between a shore core router (NCTAMS2) and the CVN connected by three satellite links (expanded data rate [XDR], medium data rate [MDR], super high-frequency [SHF]). The three satellite links were taken up and down in an order that routed traffic over different combinations of links (Figure 2). Six IP traffic types were marked with differentiated services code point (DSCP) tags. Priority-based routing was implemented on the routers using class-based weighted fair queuing so that each class of traffic enjoyed reserved capacity on all three SATCOM links and each had a preferred link when that link was available. The six traffic types used for this experiment were Naval Fires Network (NFN), Joint Services Imagery Processing–Navy Consolidated Architecture (JCA), Joint Worldwide Intelligence Communications System (JWICS), voice over Internet protocol (VoIP), video over Internet protocol (VIDoIP), and default. Each traffic type had a guaranteed minimum capacity in each SATCOM link, but each was assigned a preferred link. When the assigned link was not available, the traffic was rerouted to a different SATCOM link. The preferred link for JCA, VoIP, and default traffic was the SHF link. When the SHF link was not available, these traffic types defaulted to the XDR link. The preferred link for NFN and VIDoIP traffic was the XDR link, and the preferred link for JWICS traffic was the MDR link. When the MDR link was not available, JWICS defaulted to the SHF link.

Figures 3, 4, and 5 describe the traffic flow results through each one of the satellite links: SHF, MDR, and XDR, respectively. At t0, only the SHF link was up. Consequently, all traffic was routed via the only available link. At t1, both the SHF and the MDR

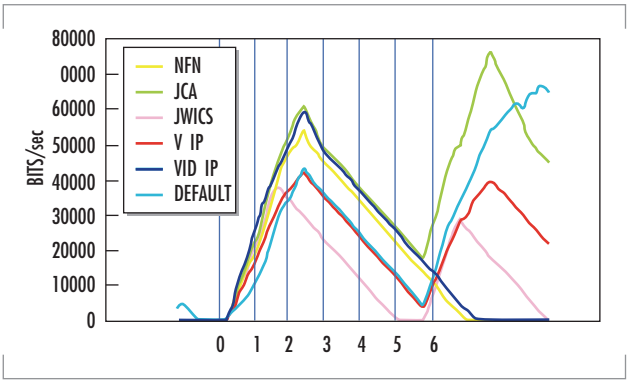


FIGURE 3. Moving-average IP traffic flow rate through the SHF SATCOM link. Traffic classes are provided a minimum guaranteed capacity in conjunction with a routing policy scheme.

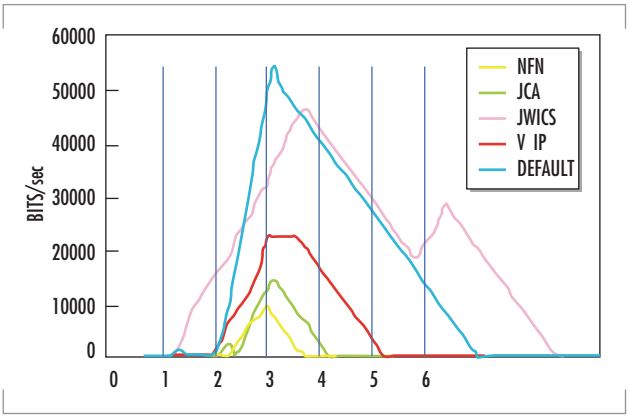


FIGURE 4. Moving-average IP traffic flow rate through the MDR SATCOM link.

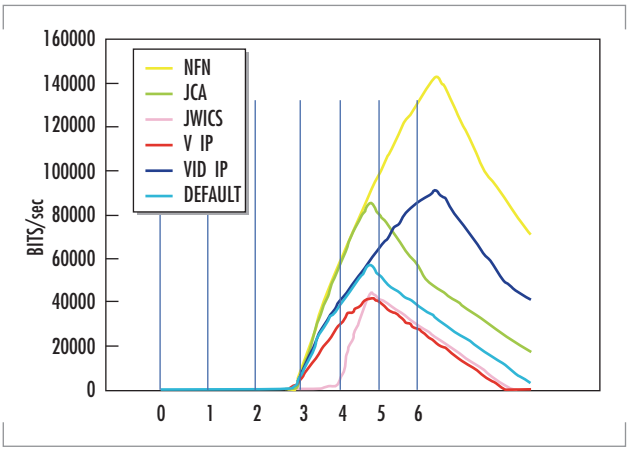


FIGURE 5. Moving-average IP traffic flow rate through the XDR SATCOM link.

links were up. At this time, JWICS traffic was routed via the MDR link since it was the preferred link. At t2, the SHF link was down and all traffic was now routed via the only available link, the MDR link. The graphs indicate link up and link down processes as a "ramp up" and "ramp down" effect, respectively. This is because the QDM tool computes a moving-average throughput. A 300-second moving average was used in this experiment. At t3, the XDR link was brought up. At this time, all traffic shifted to the XDR link except for the JWICS traffic. At t4, the MDR link was down, and all traffic was routed via the XDR link. At t5, both the SHF and the XDR links were up. At this time, JCA and VoIP traffic were routed via the SHF link, NFN and VIDoIP traffic were routed via the XDR link, and JWICS traffic was routed via the SHF link. At t6, all SATCOM links were up and all traffic was routed via the originally assigned default links. QDM data were found to be well correlated with the time logs for all three satellite links. This experiment demonstrated the ability of the network to reliably reroute traffic, depending on the availability of links with a guaranteed minimum throughput.

Overall, the LOE produced a number of significant routing design results. For example, a simple, scalable network design was accomplished with very short routing tables on all the ships, with routing tables consisting of only a default route, local-area networks, and LOS/BLOS networks. Router logs showed that ship route changes did not propagate to other ships except LOS-attached ships. Test scripts run in the global information transfer focus area showed seamless automatic routing and re-routing for global connectivity regardless of the AOR connections for ships. Global network convergence was under 30 seconds in various test scenarios.

## SUMMARY

LOE overall results supported the feasibility of a single-domain routing concept for the Fleet that is responsive to the time-critical information needs of the warfighter. LOE accomplishments included designing and validating a layered network architecture that enables seamless worldwide mobility for naval forces, validating the value of such a network for the seamless transport of time-critical targeting data, validating QoS designs and policies that distribute traffic over multiple SATCOM paths and prioritized traffic on a congested network, validating strategies for IP to the cockpit and ship-to-ship LOS/BLOS networking, and validating mechanisms for ad hoc, any-to-any connectivity for security enclaves. As one of the Navy's initial efforts to transform the concepts for network-centric warfare into operational practice, the EC5G LOE exemplifies work in SSC San Diego’s strategic imperative area of Dynamic Interoperable Connectivity.

REFERENCES

1. Pepelnjak, I. 2002. EIGRP Network Design Solutions. Cisco Press, Indianapolis, IN.
2. Vegesna, S. 2001. IP Quality of Service. Cisco Press, Indianapolis, IN.

**Daniel E. Cunningham**

Ph.D., Aerospace Engineering, University of California, San Diego, 1998

Current Work: EC5G experimentation; communications and network architecture analysis; Principal Investigator for the EC5G FY 02 LOE.

**Ayax D. Ramirez**

MS, Physics, San Diego State University, 1991

Current Work: laser physics; photonics; micro-sensors; excimer laser materials processing; non-destructive testing; network experimentation; Lead Data Analyst for the EC5G FY 02 LOE.

**Kenneth Boyd**

Ph.D., Molecular Biology, University of Arizona, 1983

Current Work: Project Manager and Lead Systems Engineer for the EC5G Project; Business Area Manager for the Advanced Network Technologies and Systems (ANTS) Program.

**Norman E. Heuss**

MS, Software Engineering, National University, 1994

Current Work: Information assurance; Joint operations, naval operations; C4I systems analysis; Information Assurance Lead for EC5G FY02 LOE.

**James Mathis**

BA, Computer Science, University of Phoenix, 1999

Current Work: Network Coordinator for the FORCEnet LOE 03-1; Deputy Director of the EC5G FY 02 LOE.

# Modeling Navy Communications Systems for NETWARS

**Thomas A. Hepner**
SSC San Diego

ABSTRACT

*The Network Warfare Simulator (NETWARS) is a joint services project under development to improve the modeling and simulation capabilities for measuring and assessing the information flow through military communications networks. It has been designated as the primary network modeling and simulation tool for the armed services. A key component for the success of NETWARS is the involvement of the military services. To help ensure the success of this program, SSC San Diego is developing communications device models of Navy-designed systems for use in NETWARS. This paper describes the NETWARS program and SSC San Diego's modeling efforts in support of this program.*

## INTRODUCTION

The Network Warfare Simulator (NETWARS) is a program jointly run by the Defense Information Systems Agency (DISA) and the Command, Control, Communications, and Computer ($C^4$) Systems Directorate (J-6) of the Joint Staff. The program was initiated in response to a need for a simulation capability to measure and assess information flow through military communications networks, determine potential sources of congestion, and assess emerging technologies on current communications networks. Prior to NETWARS, each service and government agency used specific, stovepipe approaches to analyze its communications systems. These approaches did not provide for a single, unified simulation capability that could be used by the joint services community, as well as individual services, to provide for a common network modeling simulation capability.

The NETWARS program is designed to support the following activities, all at the Joint Task Force (JTF) level and below:

- Conduct network traffic analysis
- Perform communications contingency planning
- Support wargaming and other force-on-force models
- Evaluate effect of emerging technologies on communications networks
- Support budget, acquisition, and policy deliberations

The services are supporting NETWARS by participating in the program's Architecture and Standards, Requirements, and Study groups. SSC San Diego is also supporting NETWARS by using its expertise to develop high-fidelity communications models of Navy systems for use within the program.

## NETWARS FUNCTIONAL OVERVIEW

NETWARS is designed to allow an analyst to create network communications scenarios through the use of reusable communications device models (CDM), environmental factors (such as terrain and propagation effects), military operational doctrine, and network traffic information (in the form of Information Exchange Requirements, or IERs). The program allows the communications analyst to create, evaluate, and analyze large-scale (over 5000 nodes) scenarios that include military units, organizations, and their associated communications equipment that move over

three-dimensional terrain while transmitting network communications events over simulated networks. The user can then analyze the effects of voice, video, and data traffic across the simulated communications infrastructure.

NETWARS is built using the Optimized Network Engineering Tool (OPNET) from OPNET Technologies, Inc. The NETWARS architecture consists of four primary elements: (1) Database Libraries (including Communication Device Models, Operational Facilities [OPFACs], Organizations, and IERs); (2) Scenario Builder; (3) Simulation Domain; and (4) analysis tools. Figure 1 shows the functional relationship of these components.

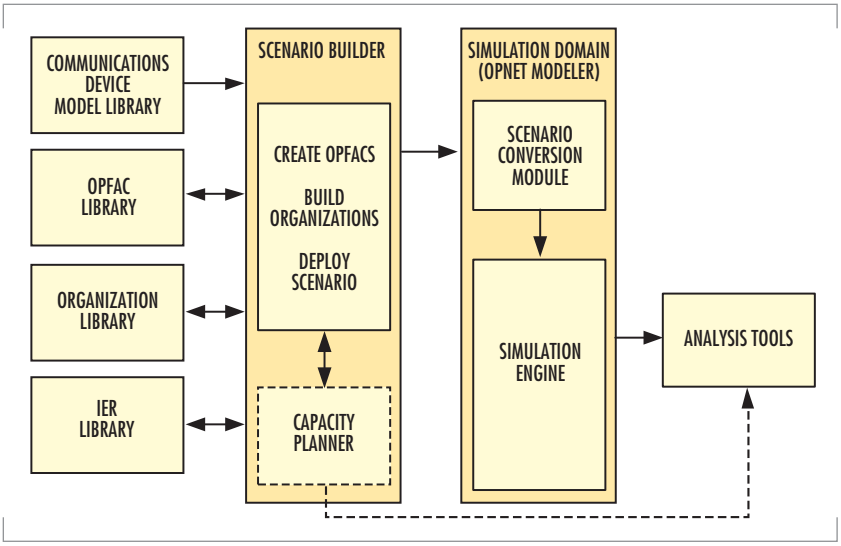


FIGURE 1. NETWARS system architecture.

## Database Libraries

The databases found within NETWARS provide the fundamental building blocks that are used to define a scenario within the program. The Scenario Builder makes use of these libraries to define detailed descriptions of the communications networks used in the scenarios. The CDMs are the basic building block of the program. They are models of actual communications device equipment and represent the protocols and functionality that are found in the actual physical device. Examples of Navy CDMs include radios, patch panels, and satellites. OPFACs can be thought of as a collection of communications devices and their connections that are logically connected. OPFACs are used by the Navy to represent systems, such as the Advanced Data Network System (ADNS) and the Global Command and Control System–Maritime (GCCS–M). Organizations consist of one or more OPFACs connected by various communications links. These links include point-to-point links, wireless links, and broadcast networks. Organizations can be assigned trajectories and can move during the scenario. IERs are used to specify the traffic that is to flow across the network. IERs define the type of traffic (voice, video, or data), its source and destination, how often the IER is sent and the size of the IER (the duration of the call for voice, and the size for video and data).

## Scenario Builder

The Scenario Builder allows the analyst to incorporate the CDMs, OPFACs, organizations, and IERs into a scenario that is translated into a software definition file that can be used by the simulation domain. The user can create and modify communications systems, create organizations, define the relationships between OPFACs and organizations, and specify link capacities, periods of failure, and recovery of OPFACs. The user also specifies the IERs that are to flow across the communications network during the simulation.

### Simulation Domain

The Simulation Domain consists of two main components, the scenario conversion module and the simulation engine. The scenario conversion module provides a common scenario description file (SDF) to the simulation engine. The SDF contains text descriptions of the scenario, OPFACs, organizations, and IERS that are used in the scenario. In theory, any simulation engine can take this file and use it to perform the communications assessment. In practice, the only simulation engine that uses this file is a commercial off-the-shelf (COTS) product built by OPNET Technologies, Inc. The simulation engine takes the SDF and processes the simulation events to obtain the network's measures of performance.

### Analysis Tools

The Analysis Tools provide a means of examining the measures of performance that were taken during the simulation. Some measures of performance that NETWARS collects include throughput, utilization, delay, blocking probability, and call/message completion rate. In addition to the built-in statistics provided by the program, the modeler can collect node-level statistics on any developed model in a NETWARS simulation.

## SSC SAN DIEGO MODELING EFFORT

### Data Circuit Modeling Effort

A significant recent SSC San Diego NETWARS modeling effort was the development of a modeling architecture for data circuit devices and systems. Data circuit devices are the backbone for the Navy's ship and shore command, control, communications, computers, intelligence, surveillance, and reconnaissance ($C^4ISR$) communications infrastructure. Data circuit systems include devices such as patch panels, multiplexers, data encryption devices that directly interface with devices such as radios, and links at the physical layer of the network. Within the NETWARS program, devices of this type are known as layer 1 circuit devices. The two key characteristics of Navy circuit devices, from a modeling perspective, are message tunneling and static multiplexing.

### Message Tunneling

Navy data circuit devices communicate with one another using protocols that often transfer data segments node-to-node a few bits at a time. When these very small segments are received by another layer 1 circuit device, they are immediately forwarded to the next device. This data-forwarding approach is often referred to as cut-through, or tunnel routing. Navy data circuit models have been designed to provide the necessary architecture to allow data to flow from packet switching, store-and-forward devices (e.g., routers) to layer 1 circuit devices, and back to another store-and-forward device. Minor propagation delays and fabric switching delays may also be specified for each data circuit device. This architecture is illustrated in Figure 2.

### Static Multiplexing

The Navy uses static multiplexing devices to define how resources such as radios, links, and satellites are to be shared. The multiplexer takes

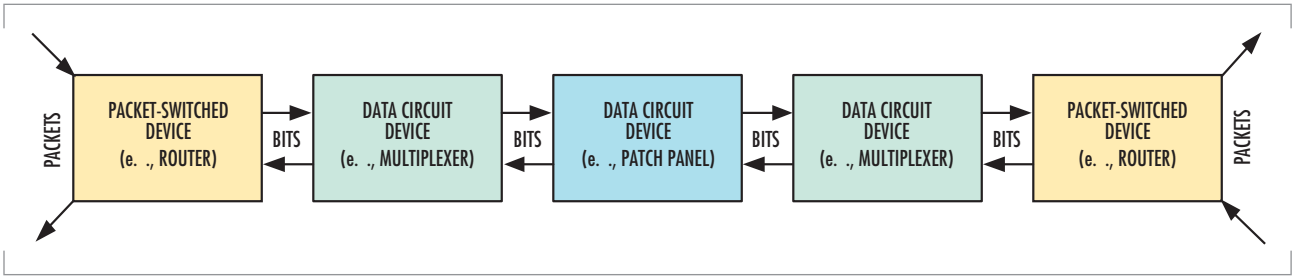


FIGURE 2. Example of message tunneling.

inputs from multiple devices and bundles these inputs, according to predefined bandwidth allocation rules, onto common output ports. Each modeled multiplexer device contains a local port and a circuit-mapping table. The mapping table is used to specify the appropriate output port and circuit number for data entering on a specific input port and circuit number. The circuit numbers are managed locally by each multiplexer. Full duplex operation is supported by the modeled multiplexers. The circuit bandwidth allocations are static, and bandwidth from idle circuits is not used for other services. Layered circuit bundling is also supported within the Navy multiplexer models. This allows a multiplexer model to include a circuit bundled from another multiplexer within its data flows. Figure 3 illustrates a layer 1 circuit device architecture example, illustrating the use of patch panels, multiplexers, radios, and satellites.

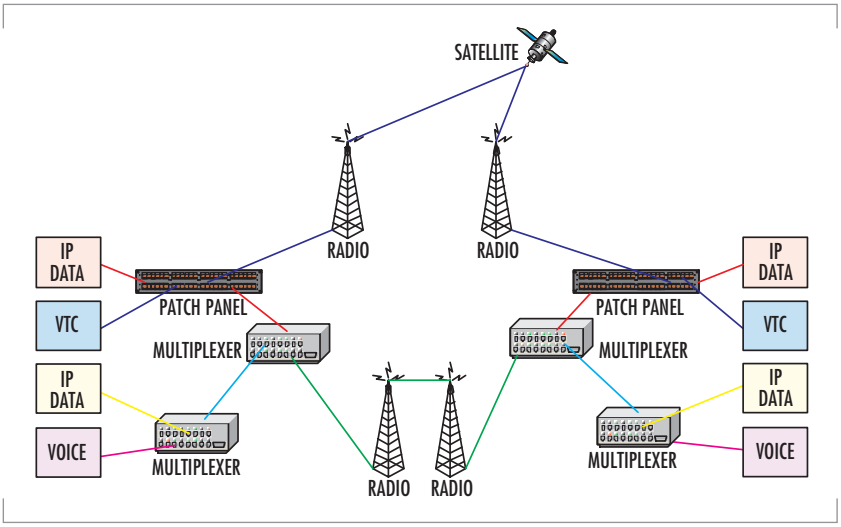


FIGURE 3. Layer 1 data circuit example architecture..

## Communications Device Modeling

The layer 1 circuit devices provide the backbone infrastructure for the development of Navy communications systems. Using this framework, we have developed additional communications device models of Navy systems. These models have been developed in accordance with the NETWARS model development guidelines, which specify the interfaces and functionality that are required of a model for it to interoperate within the NETWARS environment. The models are high fidelity, and implement the full protocol stack of the device. Some examples of Navy device models that are currently available include satellite systems (e.g., Defense Satellite Communications System and Challenge Athena) and their associated radios and end systems, such as TACINTEL, NAVMACS, STU-III, and voice phones. In all, over 60 Navy specific communications device models currently are available for use within NETWARS.

### OPFACS and Organizations

OPFACS, the fundamental building blocks of NETWARS, are built using the communications device models provided by the services, as well as commercially available device models (e.g., a Cisco router). OPFACs represent a set of co-located devices that offers a particular service. Examples of OPFACs of Navy systems currently available include the ADNS and GCCS–M. Additional OPFACs exist to support Navy modeling. OPFACs are built within the NETWARS toolkit, using the program's Scenario Builder. Device links within OPFACs are also specified within the Scenario Builder. The OPFACs can then be used to construct organizations, which for the Navy consist of ground sites, such as naval computer and telecommunications area master station (NCTAMS) sites, and classes of ships, such as carriers and cruisers. OPFACs contained within a shipboard model represent shipboard subsystems. A ship organization can contain more than 50 OPFACs. The shipboard OPFACs are organized according to infrastructure support subsystems (e.g., ADNS), as well as operational spaces and command centers (e.g., the carrier intelligence center [CVIC]). Figure 4 illustrates a simple OPFAC, while figure 5 illustrates a simple example of the infrastructure OPFACs for a DD 963 class ship organization model.

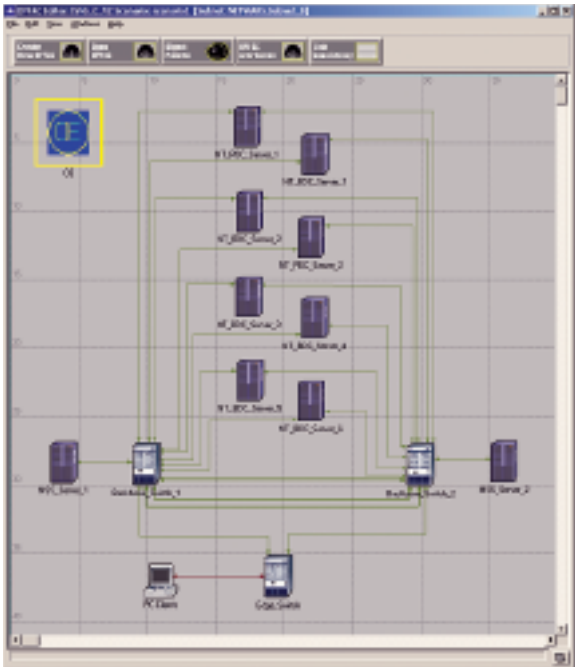

FIGURE 4. Example OPFAC, a carrier-based Secret Internet Protocol Router Network (SIPRNET).

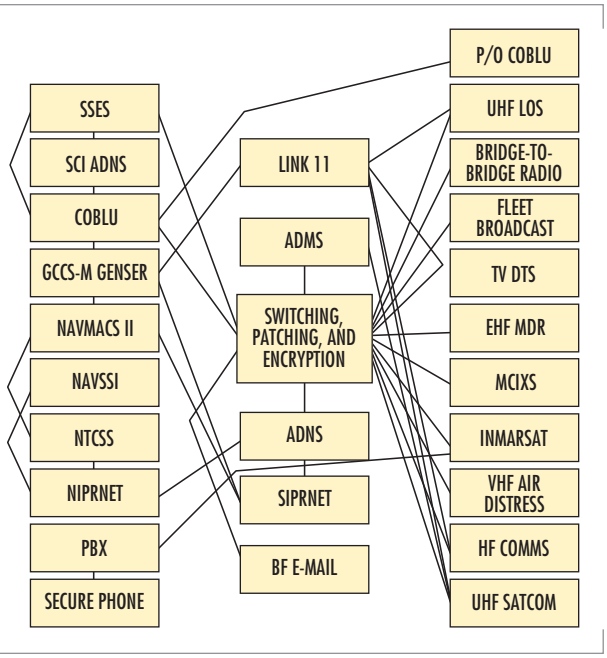


FIGURE 5. Example OPFAC infrastructure for a DD 963 class ship organization.

## CONCLUSION

SSC San Diego has leveraged its knowledge of Navy communications systems and network operability to provide accurate, high-fidelity, interoperable models of Navy communications systems to the NETWARS program. These models are now available for the Joint Task Force community, as well as the Navy, to use in accessing the current capabilities and limitations of today's networks in realistic scenarios that address mission needs for today and into the future. NETWARS, with support from the services, is able to provide a system that can now assess the current communications capabilities of systems, perform burden analysis, evaluate emerging technologies, and integrate with other modeling and simulation tools to provide our warfighters with the information needed to successfully carry out their missions.

REFERENCES

1. Dyer, C. and C. Hull. 2002. "Netwars Model Development Guide Version 1.3A," Defense Information Systems Agency, Arlington, VA.

2. Netwars Program Management Office. 2002. "Netwars User Guide Release 2002–2," Defense Information Systems Agency, Arlington, VA.
3. Murphy, W. and M. Flournoy. 2002. "Simulating Crisis Communications," *Proceedings of the 2002 Winter Simulation Conference*, pp. 954–959.
4. Mittu, R., T. Marunda, T. Hepner, A. Legaspi, E. Broyles, and J. Toomer. 2001 "Advances in Navy Data Development Efforts for the Network Warfare Simulation (Netwars) Program," Presented at *OPNETWORK 2001* (27–31 August). Washington, DC.

**Thomas A. Hepner**
MS, Computer Science, West Coast University, 1990

Current Research: Modeling and simulation of Navy communications systems; longwave ionospheric propagation; submarine communications.

# Refractivity from Clutter (RFC)

**L. Ted Rogers and Lee J. Wagner**
SSC San Diego

**Peter Gerstoft**
Scripps Institution of Oceanography

**Jeffrey L. Krolik**
Duke University, Department of Electrical and Computer Engineering

**Michael Jablecki**
Science and Technology Corporation

**ABSTRACT**

***Low-altitude atmospheric propagation conditions can change both the capability of radar systems and control settings needed to achieve optimal operation. In 1997, SSC San Diego's Atmospheric Propagation Branch began working on refractivity from clutter (RFC), a technique for estimating low-altitude propagation through processing of radar sea clutter returns. RFC is a near real-time process that uses data obtained from emissions inherent in the operations of the ship's radar and does not require expendable balloon- or rocket-borne in situ sampling instruments as used today.***

## INTRODUCTION

Modern three-dimensional (3-D) air search radars look for targets in a surveillance region that is often over 1 million cubic miles. Even today, however, such radar systems have finite resources with which to track targets. To make the most of those resources, radar systems have controls that affect which returns are detected and tracked and which returns are rejected so that operators can balance detection capability and resource loading.

When ducting is present, radar returns from sea and land clutter are tens of decibels above values associated with standard (design basis) propagation, and the result is an increase in the clutter loading. Radar operators need to know what changes in system control settings they can make that will relieve their clutter loading yet not adversely impact their ability to detect threats. To determine if targets are detectable, however, it is necessary to know the propagation loss on the path to the target. To that end, the U.S. Navy has funded a diverse range of efforts directed at estimating low-altitude propagation. Refractivity-from-clutter (RFC) is clearly a front-running strategy for providing this capability to the Fleet.

## REFRACTIVITY STRUCTURES

Figure 1 shows nominal profiles of modified refractivity as a function of height for a standard atmosphere (a), an evaporation duct (b), and two common forms of surface-based ducts (c and d). Evaporation ducts are a ubiquitous feature of the marine environment and usually (but not always; see [1]) increase the detection range to low-altitude targets. The refractivity profile within the surface layer can be determined using a "bulk model" (or "LKB" model; see [2]) to map shipboard point-measurements of air temperature, sea temperature, relative humidity, and wind speed ("bulk measurements") into a refractivity profile. The shape of the evaporation duct is exactly described by a log-linear function when the air temperature is equal to the sea temperature, and is well-approximated by the log-linear function—for the purpose of estimating propagation—under almost all other circumstances [3]. As such, the evaporation duct can be parameterized using a single parameter, the evaporation duct height. Numerous tests and papers have shown that the bulk model output is highly reliable for unstable conditions (Tsea > Tair—the normal case for open ocean), but that the models can perform

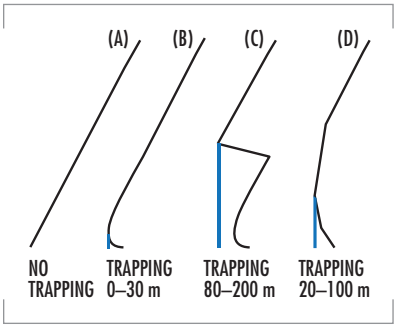


FIGURE 1. Nominal refractivity structures: (A) standard profile, (B) evaporation duct, (C) surface-based duct associated with air-mass subsidence, (D) surface-based duct associated with advection. The heavy blue line indicates the trapping (downward refracting) region.

erratically when the surface layer is stable [4], a condition that is common in coastal areas.

Surface-based ducts are less common than evaporation ducts (15% worldwide occurrence, but up to 50% of the time in the Persian Gulf), but their effects are often more dramatic. They often manifest themselves in a radar's plan position indicator (PPI) as clutter rings (e.g., see Figure 2). They also result in significant height errors for 3-D radar because the lowest elevation scans become trapped near the surface instead of refracting upward as would be expected for a standard atmosphere. Surface-based ducts are usually associated with subsidence or advection of (relatively) warm, dry air masses and cannot be characterized by bulk models. The existing means for characterizing the refractive environment is via expendables such as balloon- or rocketsondes [5].

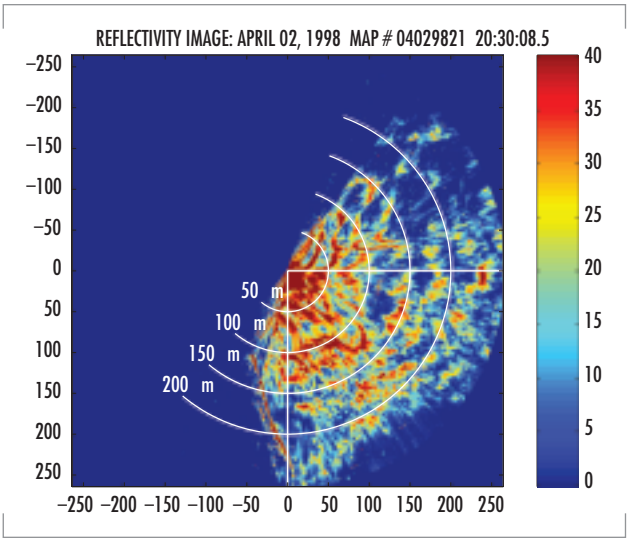


FIGURE 2. Radar clutter map showing sea clutter out to 256 km with surface-based ducting present.

## RFC EVAPORATION DUCT ALGORITHM (RFC-ED)

RFC-ED exploits results by Pappert, Paulus, and Tappert [6], whose modeling indicated that the signal for the evaporation duct is embedded in the slope of the clutter power as a function of range. RFC-ED compares the fall-off rate of clutter data from an annulus about the ship to modeled fall-off rate as shown in Figure 3. In 1998, RFC-ED was implemented on data from a test radar at Wallops Island, VA (overlooking the Atlantic Ocean) [7]. In 1999 and 2000, RFC-ED was implemented on data from the at-sea demonstration of Lockheed-Martin's Tactical Environmental Processor (TEP) system [8] onboard the USS *O'Kane* (DDG 77) and USS *Normandy* (CG 60). The Normandy results are shown in Figure 4, where most of the differences between the RFC-ED duct height estimates and those computed using the LKB model are easily within the normal errors expected with the bulk model. Virtually all exceptions are cases where the air–sea temperature difference was positive. As discussed in the preceding section, it is reasonable to question the bulk model output for the stable cases.

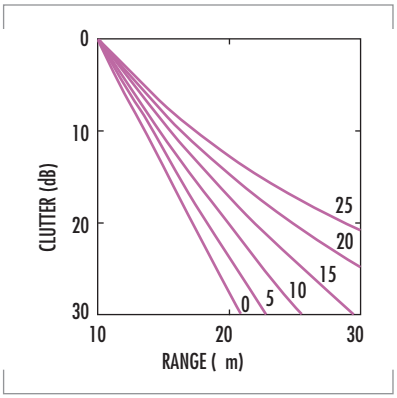


FIGURE 3. Clutter power (relative to power at 10 km) parametric in evaporation duct height.

## RFC SURFACE-BASED DUCT ALGORITHM (RFC-SBD)

Whereas inferring the evaporation duct height from sea clutter is a relatively simple parameter estimation problem, the inference of parameters describing surface-based ducts is a multi-parameter inverse problem with many similarities to inverse problems in ocean acoustics and seismic exploration. To address the surface-based duct problem, SSC San Diego teamed with Duke

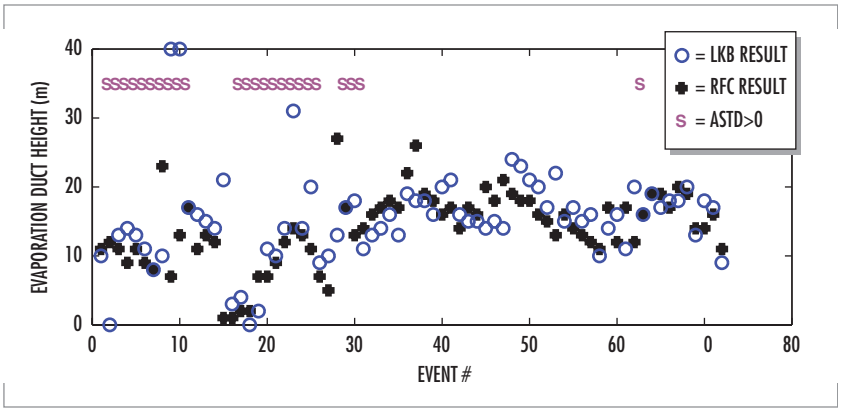


FIGURE 4. RFC-ED event series using data from USS *Normandy* (CG 60). Magenta "S" indicates matched pairs where surface layer is stable and LKB output is questionable.

University and Scripps Institution of Oceanography (SIO). From 1999 through 2001, research efforts addressed maximum a posteriori estimation [9], applying genetic algorithms [10], use of multiple elevation data [11], and particle filtering [12].

Beginning in 2002, SSC San Diego, SIO, and Duke University jointly developed a near-real-time RFC-SBD implementation that compares 20,000+ canned replica fields to observed clutter data using squared-error objective criteria. An example of the results of implementing the algorithm using data from the Space Range Radar (SPANDAR) at Wallops Island, VA, is shown in Figure 5. The vertical scan (a) shows clutter is concentrated at the lowest antenna elevations, which is consistent with ducting. The horizontal surface-scan (b) shows the classic "skip-zones" that are observed with surface-based ducts. Note that sea clutter is observed at 100+ km, whereas with a standard atmosphere, its range extent would be limited to 25 km or so. Note also that the clutter is highly azimuth-dependent, with extended range clutter present only between (roughly) the 056 and 128 markings. The observed refractivity profiles (c) show a duct. In (d) we show the observed clutter power (black), the clutter power predicted by range-dependent profiles (magenta), and the best-fitting clutter profile from RFC (blue). The effective refractive profiles from RFC associated with the best-fitting replica field are shown in (e), while the propagation loss at a height of 6 m is shown in (f).

Currently, RFC-SBD is undergoing testing using an extensive set of radar, propagation, and meteorological data from measurement campaigns conducted by the Naval Surface Warfare Center, Dahlgren Division [13].

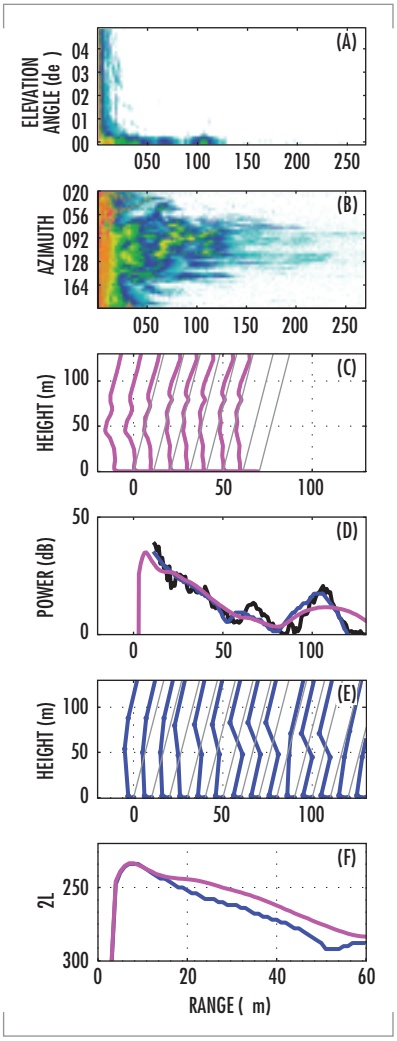


FIGURE 5. RFC-SBD (A) vertical scan, (B) horizontal scan, (C) helicopter-measured refractivity, (D) observed clutter [black], RFC best fit [blue] and clutter predicted using "c" [magenta], (E) RFC-inferred profiles, (F) two-way loss prediction for RFC [blue] and helicopter [magenta].

## RFC EMBEDDED SYSTEM

Figure 6 shows the design of the RFC embedded system. RFC is realized as an executable program that will reside within the TEP system, which is coupled to the AN/SPY-1 radar system. Lockheed-Martin developed the TEP system to passively tap into the radar system upstream of much of

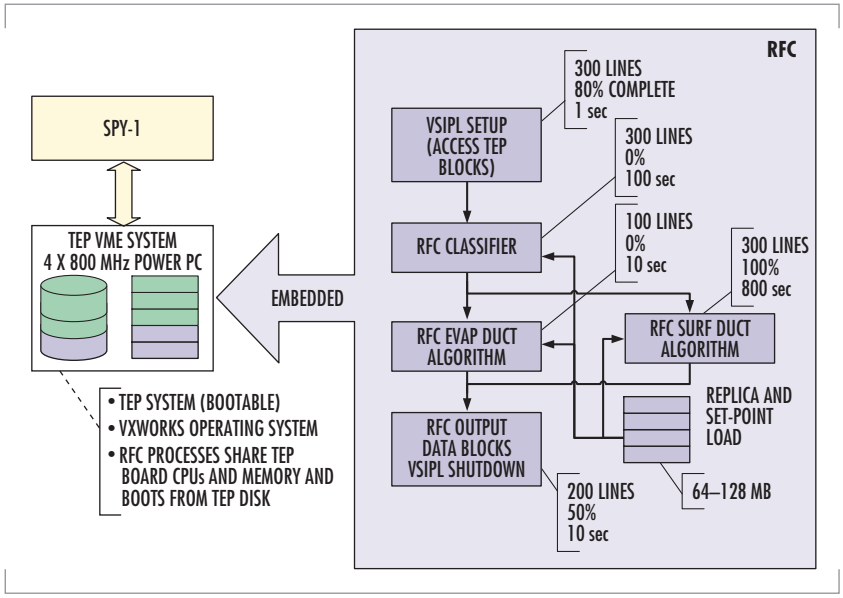


FIGURE 6. RFC embedded system.

the radar's normal processing chain and determine radar reflectivity (a normalized signal strength measure) and spectral moments from the raw data, a process that is necessary to make the data suitable for RFC.

The code for RFC is being built using the Vector, Signal, and Image Processing Library (VSIPL). VSIPL is a "C" library developed to support fast processing for embedded systems in a manner compliant with open architecture (OA). The RFC executable process begins with memory allocation and opening up views to TEP data blocks containing reflectivity information. A classifier then uses data in the first and second elevation tiers to determine if the observed clutter is consistent with evaporative ducting, surface-based ducting, or other within 10° sectors. RFC-ED or RFC-SBD are invoked as appropriate. A standard atmosphere is assumed in the instance where the clutter has been classified as "other." Once processing is complete, output data blocks are filled and memory used by the RFC processes is released. The RFC processing is consistent with having the latency of the RFC output not exceeding 15 minutes.

## OUTLOOK

A battlegroup demonstration of Lockheed-Martin's TEP system along with SSC San Diego's RFC system is planned for the 2005/6 timeframe. Additionally, other high-powered systems having vertical polarization (e.g., the Multi-Function Radar (MFR) and SPQ-9B) are also viable candidates for RFC.

REFERENCES

1. Anderson, K. D. 1995. "Radar Detection of Low-Altitude Targets in a Maritime Environment," *IEEE Transactions on Antennas and Propagation*, vol. 43, no. 6, pp. 609–613.
2. Liu, W. T., K. B. Katsaros, and J. A. Businger. 1979. "Bulk Parameterization of Air–Sea Exchanges of Heat and Water Vapor Including Molecular Constraints on the Interface," *Journal of Atmospheric Science*, vol. 36, pp. 1722–1735.
3. Eckardt, M. C. 2002. "Assessing the Effects of Model Error on Radar Inferred Evaporative Ducts," Masters Thesis, Naval Postgraduate School, Monterey, CA.
4. Blanc, T. V. 1987. "The Accuracy of the Bulk Method Determined Flux, Stability and Sea-Surface Roughness," *Journal of Geophysical Research*, vol. 92, no. C4, pp. 3867–3876.
5. Rowland, J. R., G. C. Konstanzer, M. R. Neves, R. E. Miller, J. H. Meyer, and J. R. Rottier. 1996. "SEAWASP: Refractivity Characterization Using Shipboard Sensors," (*Proceedings of the 1996 Battlespace Atmospherics Conference*). TD 2938. Naval Command, Control and Ocean Surveillance Center, RDT&E Division, San Diego, CA, pp. 155–164.
6. Pappert, R. A., R. A. Paulus, and F. D. Tappert. 1992. "Sea Echo in Tropospheric Ducting Environments," *Radio Science*, vol. 27, no. 2, pp. 189–209.
7. Rogers, L. T., C. P. Hattan, and J. K. Stapleton. 2000. "Estimating Evaporation Duct Heights from Radar Sea Echo," *Radio Science*, vol. 35, no. 4, pp. 955–966.
8. Maese, T. 2000. "Preliminary Results of At-sea Testing with the Lockheed Martin Tactical Environmental Processor," *Proceedings of Battlespace Atmospheric and Cloud Impacts on Military Operations 2000*.
9. Krolik, J. L. and J. Tabrikain. 1998. "Tropospheric Refractivity Estimation using Radar Clutter from the Sea Surface," (*Proceedings of the 1997 Battlespace Atmospherics Conference*). TD 2989. SSC San Diego, San Diego, CA., pp. 635–642.

10. Gerstoft, P., L. T. Rogers, J. L. Krolik, and W. S. Hodgkiss. 2003. "Inversion of Refractivity Parameters from Radar Sea Clutter," *Radio Science*, in press.
11. Gerstoft, P., L. T. Rogers, W. S. Hodgkiss, and L. J. Wagner. 2003. "Refractivity Estimation Using Multiple Elevation Angles," in press, *IEEE Journal of Oceanic Engineering*.
12. Vasudevan, S. and J. L. Krolik. 2001. "Refractivity Estimation from Radar Clutter by Sequential Importance Sampling with a Markov Model for Microwave Propagation," *Proceedings of the International Conference on Acoustics, Speech, and Signal Processing*.
13. Stapleton, J. K. 2001. "Radar Propagation Modeling Assessment Using Measured Refractivity and Directly Sensed Propagation Ground Truth – Wallops Island, VA 2000," NSWC/TR-01/132. Naval Surface Warfare Center, Washington, DC.

## AUTHOR INFORMATION

**L. Ted Rogers**

MS, Applied Mathematics, San Diego State University, 1990, Qualified as Surface Warfare Officer, USS *Denver* (LPD 9), 1988

Current Research: Applications of meteorological/oceanographic information in operations.

**Lee J. Wagner**

MS, Electrical Engineering, San Diego State University, 1998

Current Research: Real-time signal processing.

**Jeffrey L. Krolik**

Professor of Electrical Engineering, Duke University

Current Research: Statistical signal and sensor array processing in multipath propagation environments.

**Peter Gerstoft**

Ph.D., Civil Engineering, Technical University of Denmark, 1986

Current Research: Full field inversion methods applied to acoustic and seismic data.

**Michael C. Jablecki**

Ph.D., Biomedical Engineering, University of California, San Diego, 2002

Current Research: Refractivity from clutter and glucose sensors.

# Stochastic Unified Multiple Access Protocol for Link-16

**Allen Shum**
SSC San Diego

**ABSTRACT**

***Link-16 is the primary Department of Defense tactical data link. Although Link-16 is a very capable system, it has limitations as a dynamic networking asset. For example, Link-16 uses a pre-planning process to assign transmission capacities to platforms. The process can take several weeks, and once a network is deployed, unplanned platforms cannot join the network. Also, the capacities dedicated to absent platforms cannot be reclaimed. Designed for small networks, the current Link-16 architecture cannot scale to support the large increase of platforms projected by the Navy. The Office of Naval Research (ONR)-sponsored Dynamic Reconfiguration of Link-16 project is developing the Stochastic Unified Multiple Access (SHUMA) protocol to address these important problems. SHUMA allows Link-16 platforms to fluidly enter and exit the theater; arbitrates the statistical sharing of the channel for better network performance; operates despite jamming, dynamic topology, transmission noises, and line-of-sight constraints; and scales to support a large number of units. This paper presents the salient features of the protocol.***

## INTRODUCTION

A multiple access protocol is a set of rules that governs how distributed units access a broadcast channel such as Link-16's. Our goal is to design a Link-16 multiple access protocol that is *simple* so that it can be implemented even in the older terminals; *robust* so that it can operate well despite jamming, transmission noises, dynamic topology, and line-of-sight (LOS) constraints; *scalable* so that it can support a large number of units; *adaptive* so that it can support the dynamic entry and exit of platforms; and *efficient*. The classical multiple access problem involves a destructive channel where multiple transmissions will garble each other. Our Link-16 multiple access problem differs from the classical problem not only because of our particular objectives, but also because of capture, the LOS channel, and robustness of Link-16 applications. Capture refers to the phenomenon in which, when multiple transmissions arrive, the receiver can receive the one transmitted by the closest unit; despite simultaneous transmissions, messages can still be received. Two geographically distant units can transmit simultaneously without interference; therefore, simultaneous transmissions in Link-16 may be beneficial. To deal with the unavoidable impairments intrinsic to Link-16, such as losses resulting from transmission noise, from the LOS constraint, and from jamming, many Link-16 applications are designed to be robust so that some loss of messages is transparent. Also, Link-16 has mechanisms to retransmit lost messages for applications that require perfect reliability. Whereas restricting the number of transmitters to one is the correct paradigm for the classical problem with destructive channels and with applications that require perfect reliability, the proper objective for our Link-16 multiple access problem is to allow a few select units to transmit simultaneously so that both the robustness of applications and the spatial reuse property of the channel can be exploited.

## THE SHUMA DESIGN

Designed to scale and to be consistent with intrinsic Link-16 constraints such as LOS, high transmission noise level, and jamming, the Stochastic Unified Multiple Access (SHUMA) protocol adapts by exploiting information available at the terminal. All Link-16 platforms participate in the Precise Participant Location and Identification (PPLI) Network Participation Group and periodically transmit PPLI messages to inform

others of their presence so as to avoid being misidentified as enemy platforms. From received PPLIs, a unit can detect the presence of others and ascertain whether the units share SHUMA time slot pools. SHUMA exploits such information to enable the units to adapt and coordinate without exchanging protocol control messages.

SHUMA allows $N_i$ users to statistically share time slot i, where $1 \leq N_i$. A unit j's decision of whether to transmit during time slot i is modulated by probability $p_{i,j} = 1/N_i + (1\text{-}1/N_i)(1\text{-}(1\text{-}1/N_i)^{B_{i,j}})$. Three parameters—$N_i$, $B_{i,j}$, and $K_{i,j}$—suffice to determine this probability and to decide whether to access the time slot. The value of $N_i$ is determined dynamically from received PPLIs; the value of $B_{i,j}$ is calculated by monitoring unit j's own traffic; and the value for $K_{i,j}$ is static and is assigned. SHUMA is specified in Figure 1. (The local variable $X_{i,j}$ is defined such that $X_{i,j} = 1$ if unit j has a message to transmit and $X_{i,j} = 0$ otherwise.)

```
At reference time 0, set B_{i,j} = 0.
if (X_{i,j} = 0) /*no message to transmit*/
      begin
      (Step A) With probability 1/N_i, increment B_{i,j} by 1 if B_{i,j} is less than K_{i,j}.
      end
else
      begin /*message to transmit*/
      Generate a random number R uniformly distributed between 0 and 1.
      if (R<1/N_i)
            begin
            (Step B) Transmit a message.
            end
      else
            begin
            (Step C)
            Generate a random number R uniformly distributed between 0 and 1.
            If (R <1-(1-1/N_i)^{B_{i,j}})
            Tranmit a message and decrement B_{i,j} by 1.
            end
      end.
```

FIGURE 1. SHUMA specification.

If each of the $N_i$ units always has a message to transmit and transmits it with probability $p$, then the probability $\gamma$ that exactly one unit would transmit is $N_i p(1\text{-}p)^{N_i-1}$. The choice $p^*$ that maximizes $\gamma$ is $p^* = 1/N_i$ and is intuitively satisfying because with $p^* = 1/N_i$ the expected number of transmissions is $N_i p^* = 1$. Step B of SHUMA, transmitting with probability $1/N_i$, maximizes the probability of having a unique transmitter. Steps A and C reduce message delays while maintaining fairness of channel access. During light traffic periods when the transmission need of unit j is minimal, $B_{i,j}$ increases, thereby increasing the transmission probability when unit j's traffic load suddenly increases. $B_{i,j}$ decreases when unit j transmits a message using Step C, thereby preventing the unit from monopolizing the channel. Each unit can access its share of time slots in a way tailored to its transmission needs.

## EXAMPLE OF USE

We illustrate SHUMA through an example. Under the current approach, time slots are dedicated to units as if they will always be present at the same time and be geographically close to each other. Experience, however, indicates that whether these units will appear is uncertain and that an appreciable portion are likely to be absent. Suppose that under dedicated access the capacity is allocated equally among 100 planned units, that each unit is dedicated *one* time slot per time interval, but that only 50 units appear. Because under SHUMA the channel is statistically shared by only 50 units rather than by 100, each unit on the average can access *two* time slots per interval. Furthermore, these units might form, say, two 25-unit local groups such that each operates as if it were the only group

present. Because geographically distant units can transmit simultaneously with only minimal mutual interference, SHUMA can double the effective capacity by exploiting this spatial reuse property. Each unit can now access *four* time slots per interval without significantly increasing interference. In this example, SHUMA can increase fourfold the expected number of transmissions by each unit. SHUMA, therefore, could improve Link-16 throughput.

Unplanned units can share the capacity (dynamic entry) because the other units will scale back their rates of access to accommodate the new entrants. The capacity left behind by exited units and by units that have moved away from the vicinity can be reclaimed (dynamic exit). The remaining units can increase their rates of access. Because capacity can be allocated on a group basis rather than on a per-platform basis, SHUMA can simplify preplanning. SHUMA adapts without relying on the distribution of protocol control messages, thereby bypassing many of the difficulties associated with jamming, LOS constraints, and transmission errors; SHUMA is, therefore, robust. Because SHUMA does not require any control messages, the communication overhead does not increase as the number of units increases. As a result, it can be proved that the throughput of SHUMA is nontrivial even when the number of units is very large. The computational complexity of exercising SHUMA is independent of the number of participants (for example, a unit's decision to access the channel requires at most three logical comparisons, two random number generations, and one addition or subtraction, independent of the number of participating units), so the processing requirement does not increase significantly as the number of units increases. SHUMA is, therefore, scalable. The fact that a few lines suffice to specify the protocol testifies to its simplicity; SHUMA can be implemented in the older Link-16 terminals.

## QUEUING DELAYS

SHUMA can also reduce message delays. As an example, consider the case where eight units equally share the channel using the dedicated access approach and the case where the same units share the channel using SHUMA. In both cases, messages are generated at each unit according to the Poisson process. The expected queuing delay, the time between when a message is generated and when it is transmitted, as a function of the normalized load is shown in Figure 2. Under dedicated access, a time slot left idle cannot be reclaimed; such loss of capacity results in very high delays. SHUMA can reclaim a time slot left idle, thereby reducing message queuing delays.

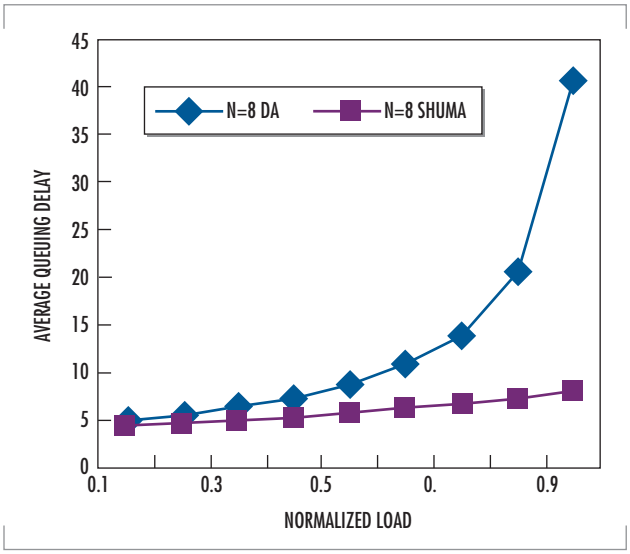


FIGURE 2. Queuing delay.

## CONCLUSION

SHUMA is a simple, adaptive, and scalable multiple access protocol designed for Link-16. It simplifies mission preplanning, supports the dynamic entry and exit of Link-16 units, and exploits the statistical nature of traffic and the spatial reuse property of the channel for higher throughput and lower message latency.

Because of its simplicity, flexibility, and scalability, SHUMA holds the promise of improving the effectiveness of Link-16.

Although the Office of Naval Research (ONR) is the sponsor for developing SHUMA, Space and Naval Warfare Systems Command (SPAWAR) PMW 101-159, the Link-16 Program Office, is implementing SHUMA in the Link-16 terminals.



**Allen Shum**

Ph.D., Electrical and Computer Engineering, University of California, Santa Barbara, 1998

Current Research: Design and evaluation of networks; stochastic analysis; design and analysis of algorithms.